iScience

CellPress
OPEN ACCESS

Article

Suppression of hepatitis B virus through therapeutic activation of RIG-I and IRF3 signaling in hepatocytes

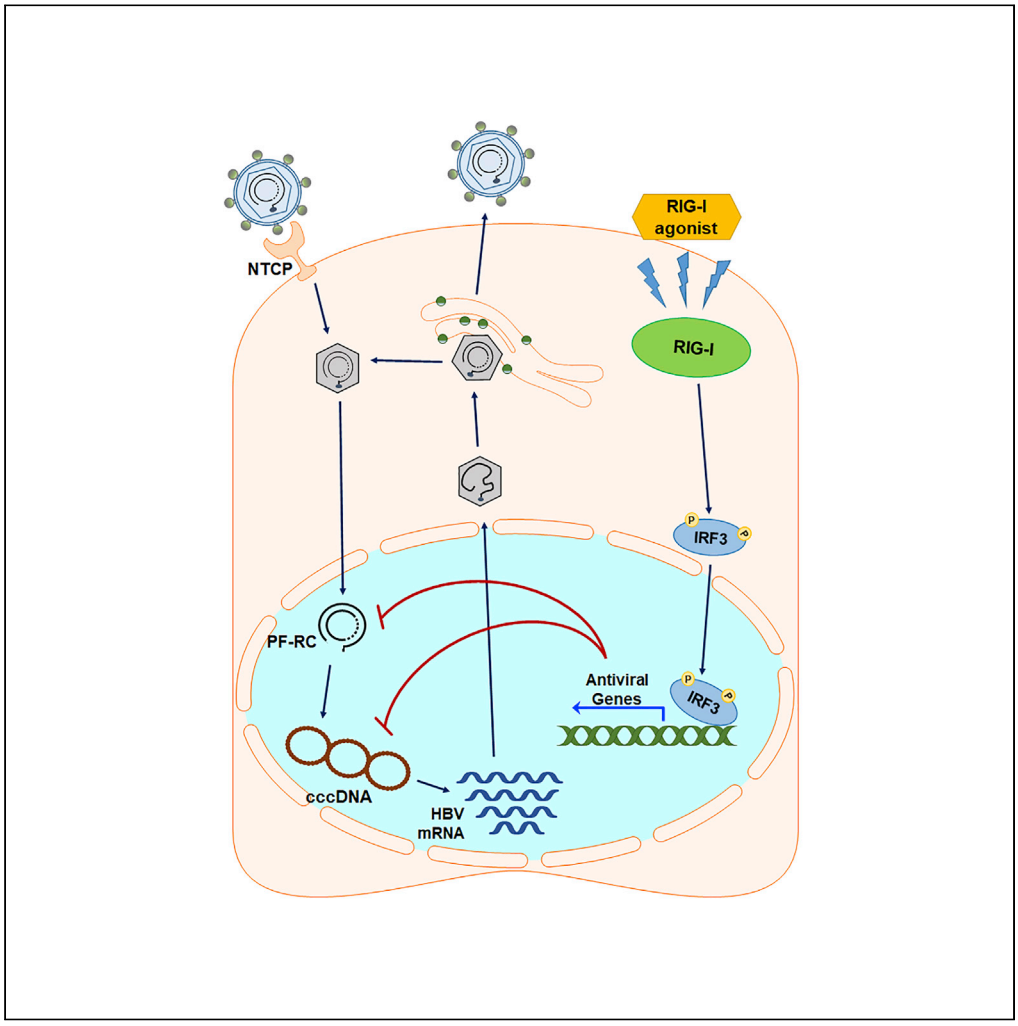

Sooyoung Lee, Ashish Goyal, Alan S. Perelson, Yuji Ishida, Takeshi Saito, Michael Gale, Jr.

mgale@uw.edu

Highlights

Hepatocyte treatment of RIG-I agonists induces IRF3 and antiviral gene expression

RIG-I agonists direct a block to cccDNA formation in early HBV infection

Administration of RIG-I agonists imparts cccDNA decay

Nucleoside analogs with RIG-I agonist is synergistic to block cccDNA formation

Lee et al., iScience *24*, 101969
January 22, 2021
https://doi.org/10.1016/j.isci.2020.101969

iScience

CellPress
OPEN ACCESS

Article

Suppression of hepatitis B virus through therapeutic activation of RIG-I and IRF3 signaling in hepatocytes

Sooyoung Lee,[1] Ashish Goyal,[2] Alan S. Perelson,[2] Yuji Ishida,[3,4] Takeshi Saito,[3] and Michael Gale, Jr.[1,5,*]

Summary

Hepatitis B virus (HBV) mediates persistent infection, chronic hepatitis, and liver disease. HBV covalently closed circular (ccc)DNA is central to viral persistence such that its elimination is considered the cornerstone for HBV cure. Inefficient detection by pathogen recognition receptors (PRRs) in the infected hepatocyte facilitates HBV persistence via avoidance of innate immune activation and interferon regulatory factor (IRF)3 induction of antiviral gene expression. We evaluated a small molecule compound, F7, and 5′-triphosphate-poly-U/UC pathogen-associated-molecular-pattern (PAMP) RNA agonists of RIG-I, a PRR that signals innate immunity, for ability to suppress cccDNA. F7 and poly-U/UC PAMP treatment of HBV-infected cells induced RIG-I signaling of IRF3 activation to induce antiviral genes for suppression of cccDNA formation and accelerated decay of established cccDNA, and were additive to the actions of entecavir. Our study shows that activation of the RIG-I pathway and IRF3 to induce innate immune actions offers therapeutic benefit toward elimination of cccDNA.

Introduction

Hepatitis B virus (HBV) is a global public health problem with more than 250 million people chronically infected worldwide. Chronic HBV infection is a leading cause of liver disease including liver cirrhosis, hepatocellular carcinoma, and liver failure such that HBV infection causes over 700,000 deaths annually (WHO, 2017) (Ott et al., 2012; Jefferies et al., 2018). HBV is a small, hepatotropic DNA virus (Marion and Robinson, 1983) that replicates in part through reverse transcription (Wang and Seeger, 1993). HBV specifically enters hepatocytes through the sodium-taurocholate cotransporting polypeptide (NTCP) receptor to replicate and produce virion (Yan et al., 2012). After entry into the hepatocyte cytosol, the viral nucleocapsid is translocated to the nucleus for disassembly and release of the viral relaxed circular (RC) DNA. In the nucleus, the RC DNA is converted to covalently closed circular (ccc)DNA that is a long-lived viral mini-chromosome serving as the main template for the synthesis of all HBV RNA transcripts including pregenomic (pg) RNA, pre-S, S, and X viral RNAs (Newbold et al., 1995; Shi et al., 2012). After synthesis the mature nucleocapsid-containing RC DNA acquires an envelope via budding at the endoplasmic reticulum (ER) and then produces progeny virion (Wang and Seeger, 1993; Seeger and Mason, 2000). A portion of the pool of mature HBV nucleocapsids is used to facilitate further cccDNA synthesis in a process called the intracellular amplification pathway (Tuttleman et al., 1986; Wu et al., 1990). This process facilitates the pool of cccDNA to be maintained as a steady-state population of 3–50 molecules per cell marking chronic infection (Seeger and Mason, 2000; Beck and Nassal, 2007; Ko et al., 2018). Removal of cccDNA from the liver either through its eradication from infected cells or depletion of infected cells is considered to be essential for HBV cure (Liang et al., 2015; Nassal, 2015; Tang et al., 2017).

Current treatment for chronic hepatitis B infection relies on two main classes of therapy, including (1) nucleot(s)ide analogs (NAs), which inhibit viral reverse transcriptase and DNA polymerase function, and (2) pegylated interferon alpha (peg-IFNα) therapy that induces innate immune defenses for suppression of viral replication and reduced HBV antigen production. Although both treatment modalities can reduce viral burden, IFN-based therapy presents considerable side effects and neither treatment is completely effective (Janssen et al., 2005). Although these therapies can suppress active viral replication, reduce cccDNA levels (Lucifora et al., 2014; Belloni et al., 2012), and can slow disease progression, they do not eliminate

[1]Center for Innate Immunity and Immune Disease, Department of Immunology, University of Washington, Seattle, WA 98109, USA

[2]Theoretical Biology and Biophysics, Los Alamos National Laboratory, Los Alamos, NM, USA

[3]Division of Gastrointestinal and Liver Diseases, Department of Medicine, Keck School of Medicine, University of Southern California, Los Angeles, CA, USA

[4]PhoenixBio Co., Ltd., Research and Development Unit, Higashi-Hiroshima, Japan

[5]Lead contact

*Correspondence: mgale@uw.edu

https://doi.org/10.1016/j.isci.2020.101969

the nuclear pool of cccDNA (Wursthorn et al., 2006; Zoulim and Durantel, 2015) and are associated with significant side effects in treated patients (Locarnini et al., 2015; Zoulim and Durantel, 2015; Kwon and Lok, 2011). The persistence of cccDNA is facilitated by long cccDNA half-life, established to be 6–22 weeks *in vivo* (Huang et al., 2020), in which lifelong treatment with antiviral therapy is required for a majority of patients to continuously suppress viral replication. Problematically, IFN-based therapy for chronic HBV is poorly tolerated and only a low frequency of treated patients show complete loss of HBsAg that defines clinical HBV cure (Dienstag, 2009; Moucari et al., 2009; Perrillo, 2009). Thus new, effective therapeutics that aim to achieve a functional cure by eradicating cccDNA are needed to treat and control chronic HBV infection (Fanning et al., 2019).

Acute viral infection typically triggers intracellular innate immune activation leading to induction of intracellular antiviral defenses. This process serves to control viral replication and spread from the site of infection, and to modulate the adaptive immune response for systemic virus control. Innate immune activation occurs via host cell sensing of viral pathogen-associated molecular patterns (PAMP) embedded in viral replication products, including viral nucleic acid. PAMPs are sensed by cellular pattern recognition receptors (PRRs). PRRs that sense virus infection include Toll-like receptors (TLR); NOD-like receptors (NLRs); intracellular DNA sensors cGAS, STING, IFI16, DAI, and others (Fernandes-Alnemri et al., 2009; Unterholzner et al., 2010); as well as the RIG-I-like receptors (RLRs) including retinoic-acid inducible gene-I (RIG-I) and melanoma differentiation antigen 5 (MDA5) (Pandey et al., 2014; Chow et al., 2018). Each PRR detects specific PAMPs derived from the incoming virus or viral replication products, while certain host cell nucleic acids can also trigger PRR signaling when produced during viral infection (Lee et al., 2019; Pandey et al., 2014). Induction of TLR, RLR, or STING signaling drives the downstream activation of latent transcription factors including interferon regulatory factor (IRF)3 and nuclear factor (NF)-κB to promote the expression of antiviral effector genes and immune regulatory genes including chemokines, IFNs, and other immune regulatory cytokines (Chow et al., 2018). Remarkably, acute HBV infection of primary human hepatocytes (PHHs) neither activates nor inhibits PRR signaling of innate immunity, thus reinforcing the notion that HBV is a "stealth" virus (Mutz et al., 2018) as previously shown *in vivo* in a nonhuman primate infection model (Wieland et al., 2004). On the other hand, strategies to activate RIG-I signaling have been shown to enhance antiviral defenses against HBV (Wu et al., 2018; Han et al., 2019), suggesting that RLR signaling can direct innate immune programs for control of HBV replication.

Previous studies have shown that RIG-I signaling in response to PAMP RNA can direct innate immune activation and antiviral defenses that suppress replication of hepatitis C virus (HCV) (Saito et al., 2008; Kell et al., 2015; Schnell et al., 2012) that also causes chronic hepatitis (Horner and Gale, 2013). The HCV PAMP is a 100-nt poly uridine/cytosine (poly-U/UC) motif with the HCV genome 3′ nontranslated region (Saito et al., 2008). When introduced into cells as a 5′ppp synthetic RNA the poly-U/UC PAMP specifically activates RIG-I to drive IRF3 activation and antiviral innate immunity that suppresses HCV infection *in vitro* (Schnell et al., 2012) and activates hepatic innate immunity *in vivo* (Saito et al., 2008). Moreover, we and others have identified small-molecule benzothiazols (Probst et al., 2017; Pattabhi et al., 2016; Bedard et al., 2012), or 5′ppp RNA ligands that bind and activate RIG-I or induce IRF3 activation and innate immunity to therapeutically suppress RNA virus infection and enhance the immune response (Dassler-Plenker et al., 2019; Hochheiser et al., 2016). Together, these previous studies show that the RIG-I pathway is functional in hepatocytes in which targeted activation of RIG-I confers potent antiviral actions that are fully operational in the liver. However, how the direct targeting and activation of RIG-I and IRF3 impacts HBV is not known.

Various innate immune programs have been shown to impact HBV infection. Beyond IFN, other pro-inflammatory cytokines have suppressive effects on HBV replication (Isorce et al., 2016) (Lanford et al., 2013) and also boost adaptive immunity against chronic HBV infection (Boni et al., 2018). Interferon-gamma and tumor necrosis factor-alpha have been shown to interfere with HBV replication at transcriptional and post-transcriptional steps and to reduce cccDNA stability (Lucifora et al., 2014; Xia et al., 2016). Thus, pharmacological innate immune activation may facilitate intrahepatic antiviral defenses and enhancement of the immune response against chronic HBV.

Here, we evaluated targeted RIG-I activation in the treatment of HBV infection *in vitro*. RIG-I signaling triggered by poly-U/UC PAMP RNA or small-molecule activator of RIG-I directed robust IRF3 activation and RIG-I-dependent antiviral actions to suppress cccDNA levels. We show that the RIG-I response through IRF3 serves to reduce the half-life ($t_{1/2}$) of cccDNA to impart cccDNA decay kinetics, and blockage of RC

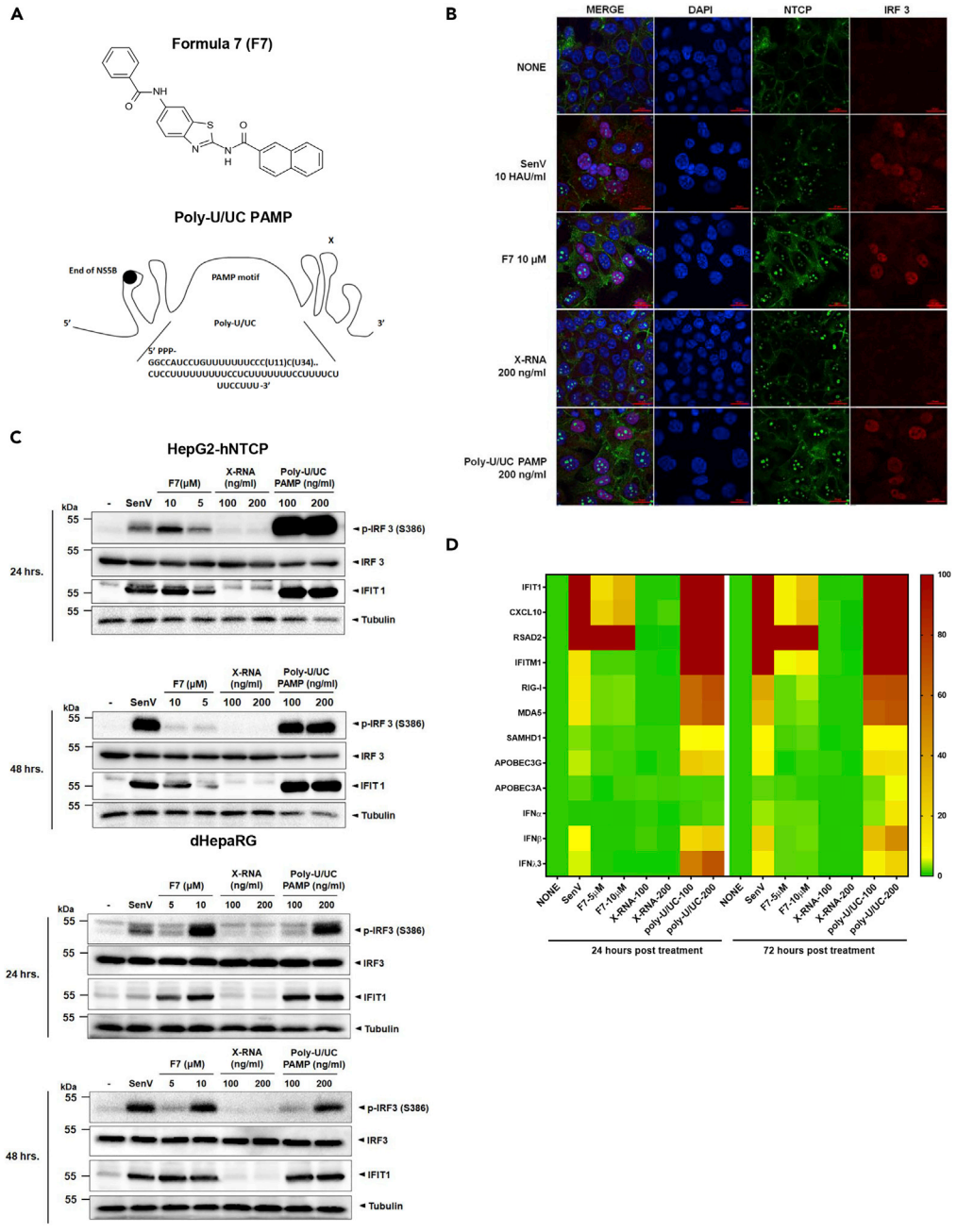

Figure 1. F7 and poly-U/UC PAMP differentially induce innate immune genes

(A) Structure of F7 and sequence poly-U/UC PAMP-RNA.

(B) Immunofluorescence analysis of IRF3 translocation. HepG2-hNTCP cells were cultured in medium containing 2.5% DMSO, infected with Sendai virus (SenV; 10 HAU/ml), or treated with F7 (10 μM), X-RNA (200 ng/mL in liposome), or poly-U/UC PAMP (200 ng/mL in liposome) for 24 h. Cells were fixed with 3% paraformaldehyde, stained by using mouse anti-hNTCP (green) and rabbit anti-IRF3 (red) antibodies, and counterstained with DAPI (blue). Scale bars, 20 μm.

(C) F7 and poly-U/UC induce IRF3 activation and innate immune gene expression. Sendai virus, F7, X-RNA, and poly-U/UC PAMP were administered to HepG2-hNTCP and dHepaRG, as indicated for 24 and 48 h. The cell lysates were resolved by SDS-PAGE and then subjected to immunoblotting. The levels of protein expression by the p-IRF3 (S386 phosphorylation active form of IRF3), IRF3 (total IRF3), and IFIT1 relative to the expression level of tubulin were determined using respective antibodies.

(D) Gene expression analysis. HepG2-hNTCP cells were administered with SenV, F7, X-RNA, and poly-U/UC-RNA as described above for 24 and 72 h; then total cellular RNA was purified from harvested cells. The levels of expression of

Figure 1. *Continued*
innate immune genes IFIT1, CXCL10, IFITM1, RSAD2, RIG-I, MDA5, SAMHD1, APOBEC3A, APOBEC3G, IFN-α, IFN-β, and IFN-λ3 were measured by qRT-PCR and normalized to the level of GAPDH expression. Each are shown as the mean fold induction over that achieved with 2.5% DMSO treatment from three independent experiments.

DNA formation and concomitant suppression of HBsAg secretion in HepG2 cells that ectopically express human sodium/taurocholate cotransporting polypeptide (hNTCP) (HepG2-hNTCP), in differentiated HepaRG (dHepaRG) cells and in PHHs. Targeting RIG-I does not promote cell toxicity. Remarkably, when combined with entecavir (ETV) and poly-U/UC PAMP, treatment rapidly depleted established cccDNA pools. Thus targeted RIG-I activation and processes that activate IRF3-directed innate immune activation may offer therapeutic approaches toward HBV cure.

Results

RIG-I and IRF3 agonists trigger innate immune activation in hepatocytes

We previously identified small-molecule agonists of IRF3 that confer innate immune activation leading to induction of IRF3-target genes and antiviral action against a range of RNA viruses (Pattabhi et al., 2016; Probst et al., 2017; Bedard et al., 2012). Based on the published structure (Iadonato et al., 2018), we produced (N-(6-benzamido-1,3-benzothiazol-2-yl)naphthalene-2-carboxamide), referred here as F7, for analyses of anti-HBV activity (Figure 1A). Similarly, we have identified a 100-nt PAMP motif within the HCV genome comprising 5′ppp and the poly-U/UC region of viral RNA that is specifically recognized by RIG-I and confers RIG-I signaling of IRF3 activation leading to antiviral gene expression (Saito et al., 2008; Schnell et al., 2012) (Figure 1A, lower). We evaluated the therapeutic actions of F7 and the poly-U/UC PAMP against HBV infection. We first treated HepG2-hNTCP cells with 10 μM F7 or 200 ng/mL poly-U/UC PAMP formulated in liposome for 24 h. Control cells were treated with DMSO or infected with Sendai virus (SenV; a potent activator of RIG-I-dependent signaling), or transfected with 200 ng/mL X-RNA negative control in liposome, a non-PAMP/non-signaling 5′ppp-containing 100 nt RNA motif from the HCV genome with similar mass to the poly-U/UC PAMP (Saito et al., 2008). Similar to SenV control, both F7 and poly-U/UC PAMP but neither DMSO nor X-RNA treatment specifically induced innate immune activation as marked by IRF3 translocation into the nucleus (Figure 1B). Immunoblot analysis demonstrated that F7 and poly-U/UC PAMP but not X-RNA treatment specifically induced IRF3 phosphorylation and the expression of IFIT1, an IRF3-target gene (Fensterl and Sen, 2011, 2015), in a dose-dependent manner in both HepG2-hNTCP and dHepaRG cells (Figure 1C). We also assessed mRNA expression across a panel of innate immune response genes, including IFNs, ISGs, and direct IRF3-target genes, for response to F7 or poly-U/UC PAMP (Figures 1D and S1). Poly-U/UC PAMP treatment also induced type I and type III IFN and ISG expression, whereas F7 treatment induced only IRF3 direct target gene expression including IFIT1, CXCL10, RSAD2, and IFITM1. This difference is consistent with the signaling properties of each molecule and the nature of IFN expression, as IFN expression relies on activation of both IRF3 and NF-kB, whereas F7 specifically activates IRF3 but not NF-kB (Bedard et al., 2012). In contrast, the poly-U/UC PAMP triggers RIG-I signaling of both transcription factors to induce IRF3-target genes, IFNs, and hence ISGs (Schnell et al., 2012; Saito et al., 2008). Notably, type I IFN, SAMHD1, APOBEC3A, and APOBEC3G, which were induced by poly-U/UC PAMP treatment, have demonstrated antiviral activity against HBV infection (Chen et al., 2014; Bonvin et al., 2006; Lucifora et al., 2014). Taken together, these results show that F7 and poly-U/UC PAMP induce innate immune activation in treated cells that initiates with IRF3 activation and the induction of IRF3-target genes.

IRF3 activation suppresses HBV cccDNA formation

To determine how IRF3 activation impacts HBV infection and production of cccDNA in infected cells, we treated HepG2-hNTCP cells with F7 or poly-U/UC PAMP (100 ng/mL [= 2.94 nM] or 200 ng/mL [= 5.87 nM]) following HBV infection. Cyclosporin A (CsA) treatment was employed as an HBV entry inhibitor antiviral control (Watashi et al., 2014). Cells were harvested 3 days post-infection (dpi), and extracts were prepared using Hirt extraction methods for isolating protein-free DNA, as shown in Figure 2A (Hirt, 1967; Guo et al., 2007). Southern blot analysis revealed that F7 and poly-U/UC PAMP treatment suppressed HBV cccDNA formation compared with the level of expression for the DMSO, or X-RNA treated controls. Additionally, the level of protein free-relaxed circular (PF-RC) DNA, which includes possible precursor forms of cccDNA, was also markedly decreased by treatment with F7 or poly-U/UC PAMP. As both F7 and poly-U/UC PAMP activate IRF3, these results link the IRF3 response with suppression of cccDNA formation in HBV-infected hepatocytes.

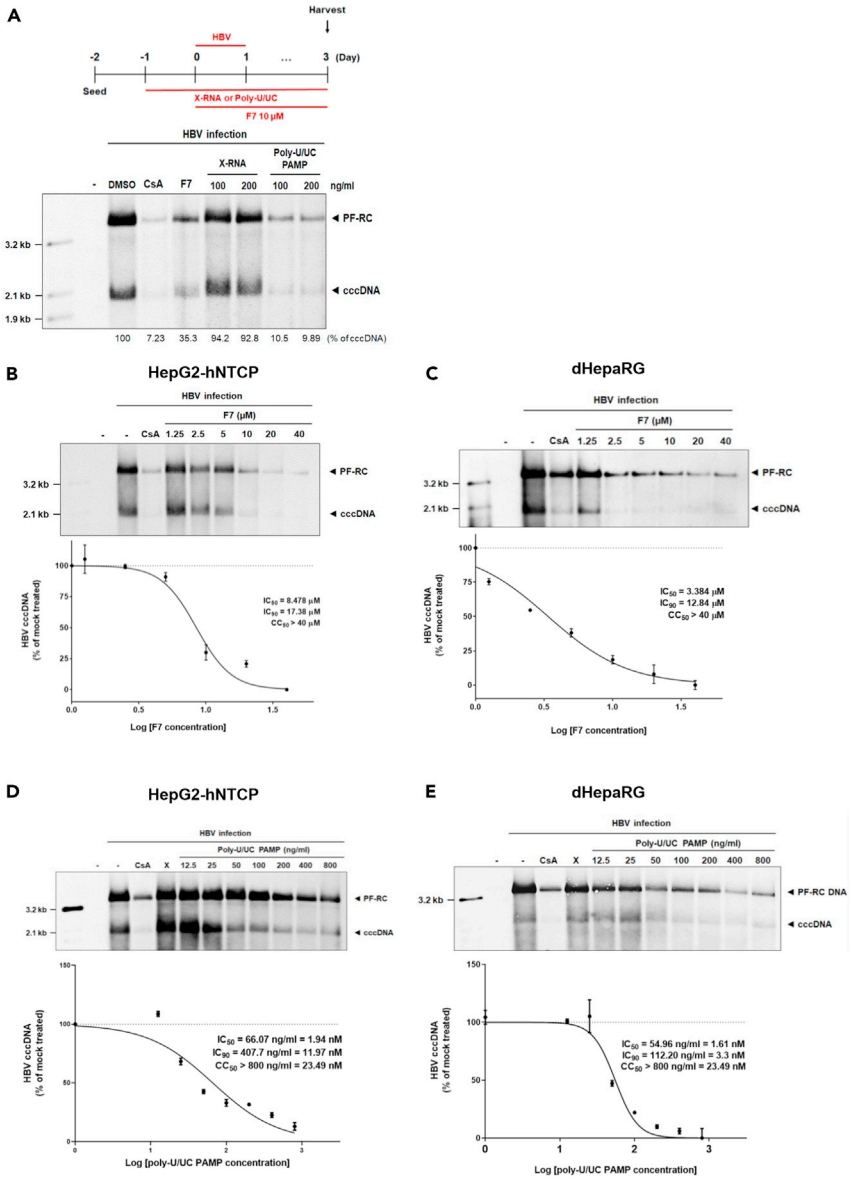

Figure 2. Therapeutic suppression of cccDNA formation

(A) Scheme of infection and treatment (upper) and Southern blot analysis (lower) to measure protein-free DNA including cccDNA. The scheme illustrates the schedule with HBV inoculum (1,000 Geq/cell) and administration of cyclosporin A (CsA), F7, X-RNA (X), and poly-U/UC PAMP. 2.5% DMSO was added to the medium at 1 day post infection (dpi). cccDNA and PF-RC DNA were harvested from HepG2-hNTCP cells using Hirt extraction method and analyzed by Southern blot analysis using an HBV-specific DNA probe. Viral protein-free DNAs (protein-free relaxed circular DNA [PF-RC DNA] and cccDNA) are noted.

(B and C) HepG2-hNTCP (B) or dHepaRG cells (C) were infected with HBV at multiplicity of infection (moi) of 1,000 Geq/cell and administered CsA (10 μM) or F7, in the indicated concentrations. For upper panels of (B and C), DNAs were isolated after Hirt extraction at 3 dpi and subjected to Southern blot analysis using as HBV-DNA probe. For lower panels of (B and C), the inhibitory effects of F7 on cccDNA formation were measured in HepG2-hNTCP and dHepaRG cells, respectively, using qPCR analysis.

(D and E) HepG2-hNTCP (D) or dHepaRG cells (E) were infected with HBV at an moi of 1,000 Geq/cell, and administered CsA (10 μM), X-RNA (X, 100ng/ml), or poly-U/UC PAMP in the indicated concentrations. For upper panels of (D and E), DNAs were analyzed using Southern blot analysis. For lower panels of (D and E), DNAs were analyzed by qPCR. IC_{90}, and IC_{50} values were calculated based on the decline of the cccDNA relative to DMSO-treated controls. IC_{90}, and IC_{50} values are the average of three experiments ± 1 SD. Cytotoxicity was determined by measuring cellular ATP content as a measure of cell viability using the CellTiter-Glo reagent. CC_{50} values shown are the average of three experiments ± 1 SD. Positions of mass markers are indicated on each Southern blot.

To further determine how the activation of IRF3 impacts the HBV replication cycle, we analyzed the expression of HBV DNA, HBV RNA, extracellular HBV DNA, and secreted HBsAg over an infection/treatment time course. As shown in Figure S2A, PF-RC DNA was first detected by 1 dpi. cccDNA synthesis occurred by 2 dpi in control-treated cells, and PF-RC and cccDNA both accumulated over the 20 dpi time course. However, the production of cccDNA was markedly suppressed in cells treated with F7 or poly-U/UC PAMP within 2 dpi. Production of pgRNA across the infection/treatment time course showed that it accumulated from 6 to 20 dpi in the non-treatment control cells but was significantly suppressed in cells treated with F7 or poly-U/UC PAMP (Figure S2B). We also measured the level of capsid-associated intracellular HBV DNA intermediates of reverse transcription produced over the HBV infection/treatment time course. We found that RC DNA, double-stranded linear (DL) DNA, and single-stranded (SS) DNA viral products accumulated from 6 to 20 dpi in control/non-treated cells. However, F7 or poly-U/UC PAMP treatment markedly decreased the levels of these DNA species. Interestingly, the level of incoming viral capsid-associated HBV DNAs (observed from 1–2 dpi) were not affected by treatment, but instead their production was suppressed within 6 dpi (Figure S2C). Suppression of HBV DNA and RNA overall was associated with significant reduction in the level of secreted HBsAg in culture supernatant from cells treated with F7 or poly-U/UC PAMP (Figure S2D). Importantly, both F7 and poly-U/UC PAMP treatment resulted in a block in *de novo* HBV production revealed by reduction of extracellular HBV DNA (Figure S2E). These results show that F7 and poly-U/UC PAMP treatment impact HBV replication at steps following cccDNA synthesis to impact transcription of viral RNA, reverse transcribed HBV DNAs, and production of progeny virions.

To assess the antiviral activity of F7 and poly-U/UC PAMP against HBV we conducted dose-response analyses. To determine the values of 90% of maximal Inhibitory concentration (IC_{90}) and half-maximal inhibitory concentration (IC_{50}), as well as the cytotoxic concentration, CC_{50}, of F7 and poly-U/UC PAMP, we used two different cell lines, HepG2-hNTCP and dHepaRG cells. Cultures were treated with increasing concentrations of F7 or poly-U/UC followed by HBV infection, then harvested at 3 dpi. Southern blot and qPCR analysis showed that cccDNA level was linearly reduced by increasing concentrations of F7 (Figures 2B and 2C) and poly-U/UC PAMP (Figures 2D and 2E). We defined IC_{90} and IC_{50} values for F7 of approximately 17.38 μM and 8.48 μM in HepG2-hNTCP cells, and 12.84 μM and 3.38 μM in differentiated HepaRG cells. The 50% cytotoxic concentration (CC_{50}), as measured by ATP release from treated cells, was over 40 μM (Figures S3A and S3B). We determined the IC_{90} and IC_{50} values of poly-U/UC PAMP to be approximately 11.97 and 1.94 nM, respectively, in HepG2-NTCP cells and 3.3 and 1.61 nM in dHepaRG cells, respectively, with CC_{50} over 23.49 nM (= 800 ng/mL) (Figures S3C and S3D).

Suppression of *de* novo HBV cccDNA synthesis

To further define inhibitory effect of F7 and poly-U/UC on cccDNA biosynthesis, we conducted time-of-addition experiments in HepG2-hNTCP and dHepaRG cells. For poly-U/UC PAMP, we conducted treatment for 24 h pre-infection (pre-treatment), from 1 to 3 dpi (post-treatment), and from 24 h preinfection onward through 3 dpi (pre/post-treatment) (Figure 3A). For F7, we conducted treatment for 24 h pre-infection (pre-treatment), 24 h initiated at the time of infection (co-treatment), from 1 through 3 dpi (post-treatment), or treatment starting at 24 h before infection and continued through 3dpi (pre/co/post-treatment) (Figure 3D). A co-treatment of CsA with virus inoculation was included as a positive control. Cultures were inoculated with HBV and harvested over the time course for assessment of cccDNA levels using Southern blot and qPCR analyses. Remarkably, we found that the synthesis of cccDNA was uniformly significantly suppressed across the poly-U/UC PAMP regimen, and to a level similar to CsA treatment, in both HepG2-hNTCP and dHepaRG cells (Figures 3B and 3C). By comparison, F7 had little effect on HBV cccDNA level when administered once pre or co-treatment but mediated a significant suppression of cccDNA levels when administered post-infection or from pre-infection throughout the 3-day course (Figures 3D–3F). These results indicate that both poly U/UC and F7 induce innate immune responses that affect cccDNA synthesis post viral entry. However, the innate immune response induced by poly-U/UC shows more sustained effect than F7.

Antiviral actions of IRF3 agonists partition to the nucleus to suppress cccDNA synthesis

To identify the step(s) of HBV cccDNA synthesis impacted by F7 and poly-U/UC PAMP treatment we assessed the level of cccDNA over a 3 dpi time course. Cells were inoculated with HBV for 6 h at 4°C, then the inoculum was removed, and the cells were rinsed and placed in 37 C media to initiate synchronous infection (time 0), at which time the cells were treated with F7 (Figure 4A), or poly-U/UC PAMP (Figures 4C) through 3 dpi. Whole-cell (W), nuclear (N), and cytoplasmic (C) extracts were harvested over the

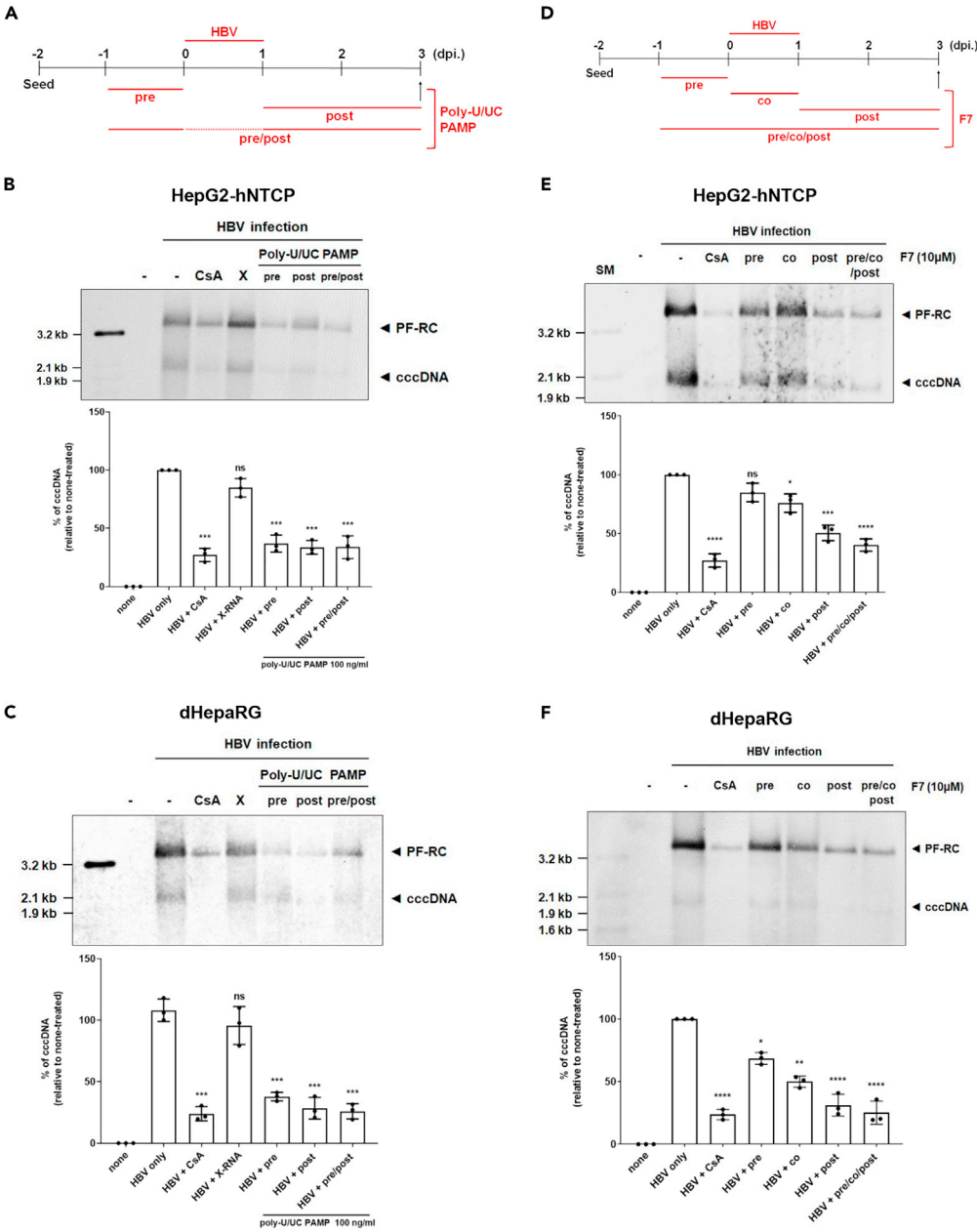

Figure 3. F7 and poly-U/UC PAMP suppress *de novo* HBV cccDNA synthesis

(A) Upper: Infection and poly-U/UC PAMP treatment schedule. Cells were treated with 100 ng/mL poly-U/UC PAMP for 24 h before (pre), for 48 h after HBV infection (post), or for 72 h (pre/post).

(B and C) At 3 dpi cells were harvested and Hirt extracts were prepared. (B) HepG2-hNTCP cells and (C) dHepaRG cells were analyzed by Southern blot (upper) and qPCR (lower). For qPCR analysis, values from DMSO-treated control were set to 100%, respectively, and data are shown as mean ± standard deviations (SD) percentage of cccDNA in control samples. ***p < 0.005, and ns, non-significant. CSA, Cyclosporin A; X, X-RNA.

(D) HBV infection and F7 treatment schedule. Cells were treated with F7 (10 µM) for 24 h before (pre), 24 h during the time of infection (Co), 48 h after infection (post), or 96 h (pre/co/post).

(E and F) At 3 dpi, the cells were harvested and Hirt extracts prepared. HepG2-hNTCP (E) and dHepaRG cells (F). Upper panels show Southern blot analysis. Lower panels show qPCR analysis and percent of cccDNA remaining in treated cells compared with control cells. Values from DMSO-treated control cultures were set to 100%.

Data was presented as mean ± standard deviations (SD), *p < *0.01*, **p < *0.005*, ***p < *0.001*, ****p < *0.0001*, ns = non-significant. CsA served as a treatment control. For Southern blots the position of mass markers are indicated. CSA, Cyclosporin A; X, X-RNA.

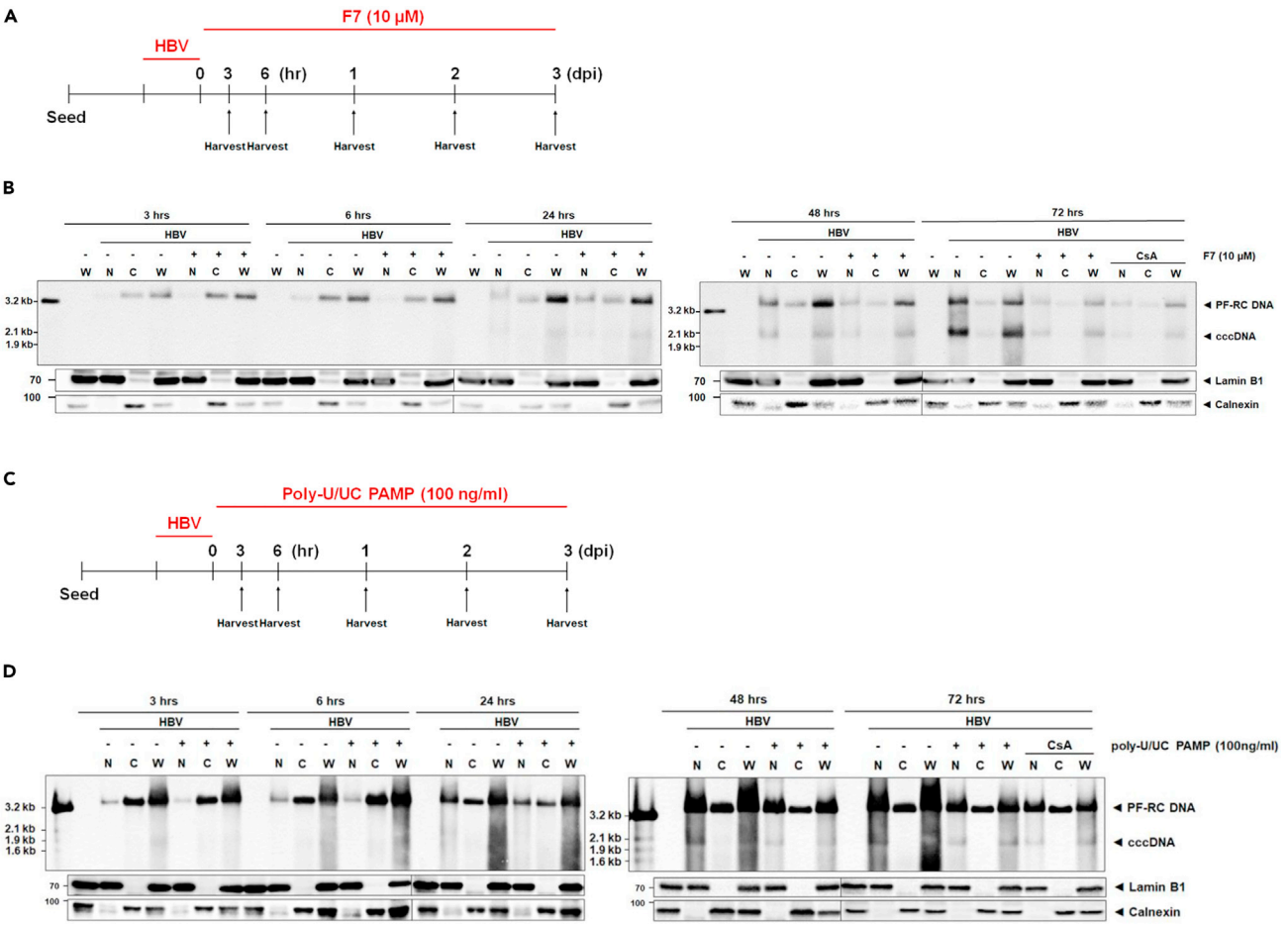

Figure 4. Subcellular compartment analysis of antiviral activity

(A and C) Scheme of HBV infection with F7 treatment (A) or poly-U/UC PAMP treatment (C). HepG2-hNTCP cultures were inoculated with HBV at moi 1,000 Geq/cell for 24 h. On treatment day 0 the cultures received F7 (10 μM) or poly-U/UC PAMP (100 ng/mL). Cells were harvested for production of Hirt extracts at each time point shown through 3 days. Parallel cultures were harvested for western blot analysis to monitor Lamin B1 and Calenxin as markers of whole-cell lysate and cytosol, respectively. CSA, cyclosporin A control treatment.

(B and D) DNA was analyzed by Southern blot using HBV-specific DNA probe. Viral protein-free DNAs (PF-RC DNA and cccDNA) are indicated. The position of mass markers is indicated. Lower panels show western blot of Lamin B1 and Clanexin abundance. CSA, cyclosporin A control treatment.

time course, at 3 and 6 h post-infection (hpi), and daily over 1–3 dpi, and PF-RC and cccDNA abundance was analyzed by Southern blot. As shown in Figure 4B, PF-RC DNA was detected in cytoplasmic and whole-cell lysate fractions from 3 hpi and in nuclear fraction by 6 hpi, but accumulation was reduced after 2–3 dpi from F7 treatment. cccDNA was detected by 1 dpi in non-treated cells, but cccDNA accumulation was delayed and reduced in cells treated with F7. For poly-U/UC PAMP treatment we also harvested cells over a similar time course (see Figure 4C). Assessment of HBV DNA in subcellular fractions also showed that PF-RC DNA was present early in non-treatment cells at 3 and 6 hpi in the whole-cell and cytoplasmic extracts with levels accumulating in the nuclear fraction thereafter. Nuclear PF-RC DNA levels were reduced in cells treated with poly-U/UC PAMP from 1–3 dpi concomitantly with reduction of cccDNA in treated cells (Figure 4D). These results indicate that the inhibitory effects of F7 and poly-U/UC on HBV cccDNA biosynthesis occurs in the nucleus at 1–3 dpi during treatment to possibly impact the conversion step of PF-RC DNA to cccDNA early in the HBV replication process.

The IRF3 activation restricts the stability of HBV cccDNA alone and in combination with ETV

To determine how the host response to IRF3 activation suppresses HBV cccDNA levels, we evaluated the influence of F7 or poly-U/UC PAMP single treatment and the combination of ETV/F7 or ETV/poly-U/UC

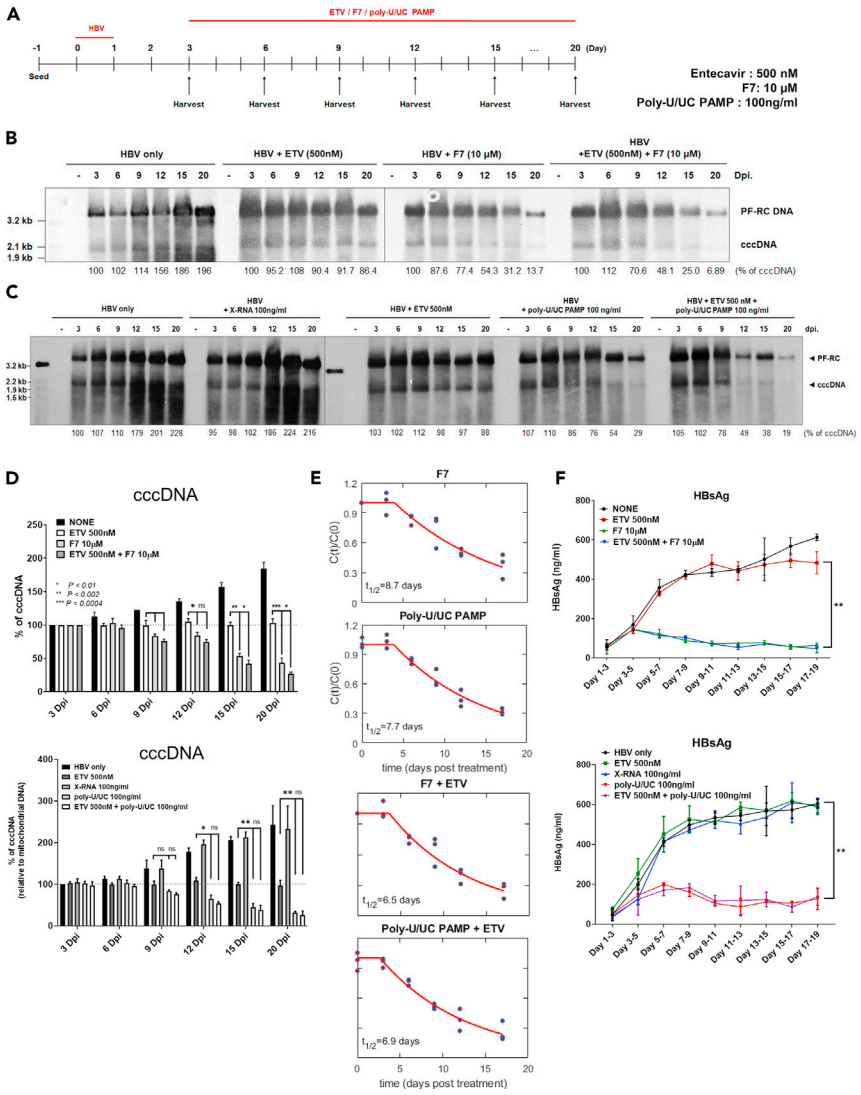

Figure 5. F7 and poly-U/UC PAMP treatment directs HBV cccDNA decay

(A) HBV infection and treatment schedule. HepG2-hNTCP cells were infected with HBV at moi of 1,000 Geq/cell, incubated for 24 h, and media was replaced. On day 3 the cells were harvested or treated with DMSO, ETV (500 nM), F7 (10 μM), poly-U/UC (100 ng/mL), or with ETC combination with F7 or poly-U/UC PAMP. Cells were harvested at the indicated points over a 20-day time course.

(B and C) DNA was isolated by Hirt extract and subjected to Southern blot analysis using an HBV-specific DNA probe. Percentage values below each lane indicate the relative amount of cccDNA compared with day 3 control before each treatment. The position of mass markers is indicated.

(D) cccDNA levels were measured by qPCR. Relative cccDNA values to mitochondrial DNA (MT-CO3) are shown. Statistical significance was determined using Student's t test. Data are presented as mean ± standard deviation (SD), *p < *0.01*, **p < *0.005*, ***p < *0.001*, ns = non-significant.

(E) Half-life of cccDNA from qPCR analyses was estimated from the simultaneous fitting of three replicates under each treatment strategy. C(t) is the % values of cccDNA at time "t" post-treatment, C(0) is the % values of cccDNA at the start of the treatment.

(F) HBsAg across the time course for each treatment series. Statistical significance was determined using Student's t test. Data are presented as mean ± standard deviations (SD), **p < *0.005*, ns= non-significant.

PAMP on cccDNA decay kinetics. To assess cccDNA decay we compared F7 and poly-U/UC PAMP treatment of HBV-infected cells with ETV treatment, starting at 3 dpi with treatment maintained through 20 dpi via daily media change with fresh ETV, F7, or poly-U/UC PAMP (Figure 5A). ETV is an NA that

prevents the reverse transcription and replication of new synthesized HBV DNAs, thereby blocking the replenishment of cccDNA from intracellular amplification. ETV was applied to HBV-infected cells at a 100-fold IC_{50} dose thereby allowing for the measurement of cccDNA half-life under conditions in which levels are sustained from early established cccDNA pool but not counterbalanced by the newly produced cccDNA (Langley et al., 2007). Cells were then harvested over a treatment time course, and DNA extracts were analyzed by Southern blot and qPCR assay. As shown in Figure 5B, cccDNA levels modestly increased over the infection time course in non-treatment control cells. Cells from ETV-treated cultures stably maintained cccDNA levels over the time course at levels similar to 3 dpi cultures, demonstrating sustained and stable cccDNA of over 20 dpi in our *in vitro* culture system, well in line with the reported cccDNA half-life ($t_{1/2}$) of greater than 40 days (Figure S4, Ko et al., 2018; Huang et al., 2020). However, F7 single treatment stimulated the decay of cccDNA as measured by Southern blot analysis (Figure 5B), and qPCR (Figure 5D). F7 mono-treatment reduced the $t_{1/2}$ of cccDNA, whereas the combination of ETV with F7 further enhanced their antiviral effects to reduce cccDNA abundance and persistence to barely detectable level by 20 dpi (Figures 5B and 5D). We also found that a mono-treatment with single administration of poly-U/UC PAMP reduced the cccDNA abundance, whereas it continued to accumulate in cells treated with X-RNA control, as analyzed by Southern blot (Figure 5C). The inhibitory effect on cccDNA levels by poly-U/UC PAMP was also confirmed by qPCR assay (Figure 5D). We also found that poly-U/UC PAMP in combination with ETV served to reduce cccDNA abundance and persistence across a treatment time course over ETV or poly-U/UC PAMP alone, with cccDNA being barely detectable after 20 dpi with co-treatment (Figure 5C). Mathematical modeling revealed that combination of F7 or poly-U/UC treatment with ETV reduced the cccDNA $t_{1/2}$ resulting from monotreatment compared with each respective co-treatment from an average of 8.7 to 6.5 days (F7) and from 7.7 to 6.9 days (poly-U/UC PAMP) (Figures 5E and S5). Neither ETV nor X-RNA treatment of cells had any effect on the production and secretion of HBsAg. However, poly-U/UC PAMP and F7 mono- and combination treatments suppressed HBsAg secretion (Figure 5F). Thus, F7 and poly-U/UC PAMP impart the therapeutic decay of established cccDNA. Moreover, combination treatment of F7 and poly-U/UC PAMP with ETV imparts additive antiviral actions to suppress cccDNA $t_{1/2}$ and persistence from weeks (Huang et al., 2020; Ko et al., 2018) to less than 7 days.

Suppression of HBV cccDNA by IRF3 activation is RIG-I dependent

To ascertain whether the activation of IRF3 and suppression of cccDNA in HBV-infected cells by F7 or poly-U/UC PAMP treatment was dependent on RIG-I rather than occurring as an off-target effect of IRF3 agonist treatment, we produced HepG2-hNTCP cells expressing non-targeting guide RNA (HepG2-hNTCP-NT), or guide RNA for knockout (KO) of RIG-I expression (HepG2-hNTCP-RKO) or MDA5 (HepG2-hNTCP-MKO) using CRISPR-Cas9 genome editing technology. Immunoblot analysis of the different cell populations shows that HepG2-hNTCP-RKO or HepG2-hNTCP-MKO cells do not express detectable levels of RIG-I or MDA5, respectively (Figure S6). Treatment of cells with F7 (Figure 6A) or poly-U/UC PAMP (Figure 6B) shows that the HepG2-hNTCP-RKO cells do not respond to treatment, whereas HepG2-hNTCP-NT control cells and HepG2-hNTCP-MKO cells fully respond to F7 to accumulate phosphorylated/activated IRF3 concomitant with expression of IFIT1. HepG2-hNTCP-MKO cells serve as an RLR KO control to reveal the specificity of F7 and poly-U/UC PAMP for triggering RIG-I-dependent IRF3 activation (Saito et al., 2008). We next infected each cell population with HBV followed by a single treatment with F7 or poly-U/UC PAMP at 1 dpi. Cells were harvested at 3 dpi for Southern blot analysis of cccDNA levels. Parallel cultures of each cell population were treated with DMSO or single-dose X-RNA (negative control) or with CsA as a treatment control. F7 treatment reduced cccDNA levels in HepG2-hNTCP-NT and HepG2-hNTCP-MKO cells but not in HepG2-hNTCP-RKO cells (Figure 6C). Similarly poly-U/UC PAMP suppression of cccDNA was dependent on RIG-I, as cccDNA was suppressed by poly-U/UC PAMP treatment in HepG2-hNTCP-NT and HepG2-hNTCP-MKO cells but not in the HepG2-hNTCP-RKO cells (Figure 6D). These results demonstrate that the antiviral actions of F7 and poly-U/UC PAMP against HBV specifically signal through RIG-I, defining each as a RIG-I agonist that activates IRF3 to impart suppression of cccDNA.

RIG-I signaling of IRF3 activation suppresses HBV infection in primary human hepatocytes

To validate the antiviral actions of RIG-I signaling of IRF3 activation by poly-U/UC PAMP we assessed HBV infection in non-immortalized and terminally differentiated PHHs that retain the expression of hepatocyte marker genes at a level comparable to that of human liver tissue. We treated PHH cultures over a poly-U/UC PAMP dose-response and assessed innate immune activation. Treatment of PHH cultures with 50–200 ng/mL poly-U/UC PAMP induced IRF3 activation marked by accumulation of phosphoserine 386 IRF3 and IFIT1 expression. Treatment with 100 ng/mL X-RNA did not induce innate immune activation of PHH, but cells

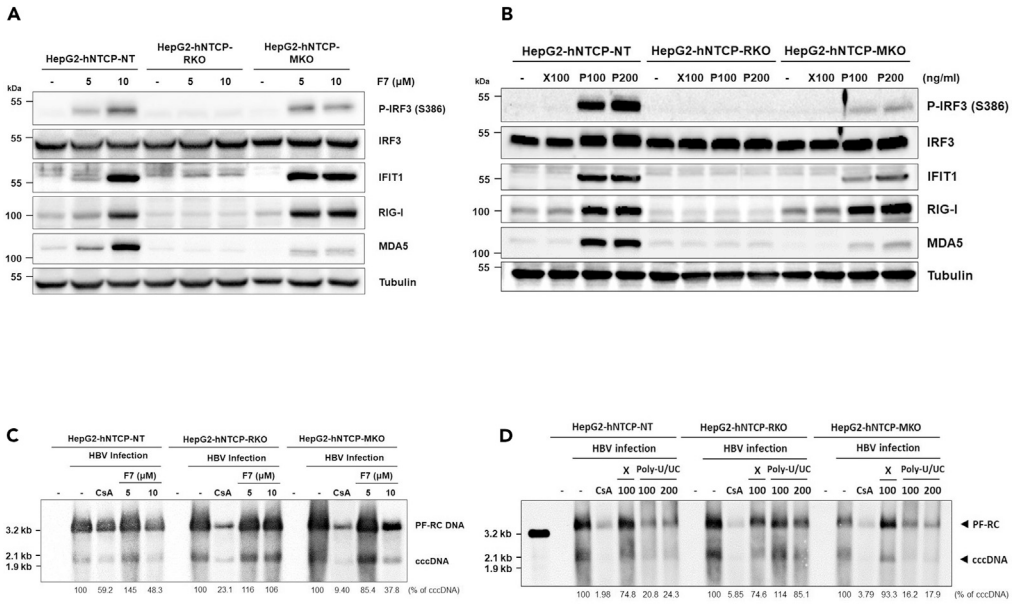

Figure 6. F7 and poly-U/UC PAMP specifically signal IRF3 activation through RIG-I to suppress HBV cccDNA

(A) F7 was administered for 24 h to HepG2-hNTCP-NT, RKO, and MKO cells. Cells were harvested and analyzed by immunoblot. The levels of protein expression by p-IRF3 (S386 phosphorylated), IRF3 (total IRF), IFIT1, RIG-I, and MDA5 relative to the expression level of tubulin were determined using respective antibodies.

(B) HepG2-hNTCP-NT, RKO, and MKO cells were treated with 100 ng/mL X-RNA (X) or 100 ng/mL or 200 ng/mL poly-U/UC PAMP (P) for 24 h. Cells were harvested and analyzed by immunoblot as in (A).

(C and D) Cells were infected with HBV at moi of 1,000 Geq/cell. After 24 h cultures were treated with DMSO (-; negative control), CsA (treatment control), (C) 10 μM F7 or (D) X-RNA or poly-U/UC PAMP. Three days later the cells were harvested and Hirt extracts were prepared and subjected to Southern blot analysis using as HBV-DNA probe. The position of mass markers is indicated. Values beneath each lane show percent cccDNA remaining compared with control treatment.

were fully responsive to acute infection with SenV control (Figure 7A), demonstrating that PHHs harbor an intact RIG-I pathway. Moreover, PHH treatment with poly-U/UC PAMP, but not X-RNA, robustly induced innate immune gene expression (Figure 7B). We then evaluated cccDNA levels in HBV-infected PHH treated with poly-U/UC PAMP. PHH cultures were infected with HBV and subject to a single treatment with poly-U/UC PAMP at 1 dpi. Cells were harvested at 3 dpi and DNA was extracted and subject to Southern blot analysis. As shown in Figure 7C, treatment with poly-U/UC PAMP suppressed cccDNA levels in the infected PHH to levels similar to CsA treatment. Thus, poly-U/UC treatment to trigger RIG-I signaling of IRF3 and innate immune activation directs a response in HBV-infected PHH that suppresses cccDNA. These results demonstrate the efficacy of therapeutic targeting of the RIG-I pathway for viral control in relevant primary cells of HBV infection.

Discussion

Persistence of cccDNA in the nucleus of HBV-infected hepatocytes is key to mediating chronic HBV infection, wherein recent analyses indicates that a given pool of cccDNA has a $t_{1/2}$ *in vivo* of approximately 5–21 weeks (Huang et al., 2020). Problematically, current therapies for the treatment of chronic HBV infection neither significantly reduce nor eliminate cccDNA (Zoulim and Durantel, 2015; Maynard et al., 2005; Werle-Lapostolle et al., 2004). Members of the current NA class of HBV therapeutics are administered for prolonged, often lifelong periods to keep patients virally suppressed. Moreover, these therapies are leaky in their ability to completely shut down viral replication, such that the nuclear cccDNA pool (Huang et al., 2020) still persists after long-term treatment (Werle-Lapostolle et al., 2004; Zoulim and Locarnini, 2009; Gish et al., 2012), Importantly however, it has been demonstrated that suppression of cccDNA during acute HBV infection can occur through a cytokine-driven non-cytolytic mechanism directed by IFN-α, IFN-γ, or tumor necrosis factor alpha linked with expression of APOBEC3 deaminases (Lucifora et al., 2014; Xia et al., 2016). Pharmacological induction of intrahepatic cytokine responses has been coined as an ideal curative approach to chronic hepatitis B (Chang et al., 2012). While this approach leverages the innate

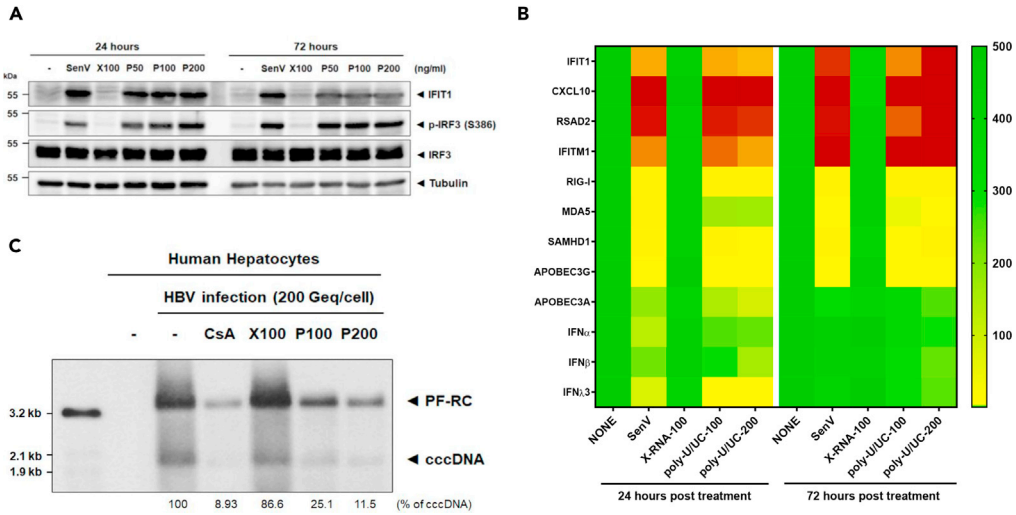

Figure 7. Suppression of cccDNA in primary human hepatocytes

(A) PHHs were cultured alone or were treated with 100 ng/mL X-RNA (X100), or 50 ng/mL (P50), 100 ng/mL (P100), or 200 ng/mL (P200) poly-U/UC PAMP, or were infected with SenV (control) and harvested 24 and 72 h later. The cell lysates were analyzed by immunoblot for p-IRF3 (S386 phosphorylated), IRF3 (total IRF3), IFIT1, and actin (control) using respective antibodies.

(B) PHH cultures were cultured alone or were treated with 100 ng/mL X-RNA (X100), or 100 ng/mL (P100) or 200 ng/mL (P200) poly-U/UC PAMP, or were infected with SenV (control) and harvested 24 and 72 h later. Cells were harvested and RNA was extracted and analyzed by RT-qPCR to measure the expression levels of the indicated innate immune genes normalized to the level of GAPDH expression. Values are shown on the heatmap as mean fold induction over non-treated cells from three independent experiments.

(C) PHH cultures were inoculated with HBV at moi of 200 Geq/cell. 24 h later the cultures were treated with CsA (treatment control; 10 μM), 100 ng/mL X-RNA (X100), or 100 ng/mL (P100) or 200 ng/mL (P200) poly-U/UC PAMP. Three days later the cells were harvested, DNA isolated by isolated Hirt extraction, and analyzed by Southern blot using an HBV-specific probe. Viral protein-free DNAs (PF-RC DNA and cccDNA) are noted. Values under each lane show the percent remaining cccDNA compared with non-treated control. The positions of mass markers are shown on the left.

immune and immune modulatory signaling programs driven by specific cytokines to induce the expression of genes whose actions can suppress cccDNA, cytokine therapy for treatment of chronic HBV faces the obstacles of systemic toxicity from the broad off target, nonhepatic actions of cytokine treatment (Kwon and Lok, 2011; Locarnini et al., 2015), underscoring the need for target-directed therapeutic strategies that can also be coupled with current NA therapeutics against HBV.

We demonstrate that targeting RIG-I and the RLR pathway to activate IRF3 via the F7 small-molecule and poly-U/UC PAMP agonists of RIG-I delivered to hepatocytes directs a specific RIG-I-dependent innate immune response through IRF3 that effectively suppresses HBV cccDNA in a cell culture model of HBV infection. Furthermore, mechanistic studies show that the administration of F7 or poly-U/UC PAMP suppresses *de novo* biosynthesis of cccDNA and enhanced cccDNA degradation rather than inhibiting the production of newly synthesized HBV rcDNA as current NA HBV drugs do. Administration of F7 and poly-U/UC PAMP induces IRF3 activation and expression of IRF3-target genes (Figure 1). Thus, the underlying mechanisms of F7 and poly-U/UC PAMP to suppress cccDNA likely involve the actions of IRF3-target genes to block cccDNA synthesis and impart actions that facilitate the destabilization and degradation of cccDNA to deplete it from the infected cell. We note that F7 treatment of cells does not induce expression of type I or III IFN, owing to the RIG-I activation properties of this class of compounds that do not impart signaling to NF-kB but instead exclusively activate downstream IRF3 (Bedard et al., 2012; Probst et al., 2017). Thus, in the case of F7 the antiviral actions to suppress cccDNA operate independent of IFN actions but through IRF3-responsive genes. Our results show that poly-U/UC PAMP also induces robust IRF3-target gene expression as well as a low level of IFN that can induce ISGs. Among these are the APOBEC3 genes, known antiviral effectors against HBV replication (Turelli et al., 2004; Bonvin et al., 2006). IRF3 activation drives the expression and production of various immune modulatory cytokines and chemokines, including CXCL10, a chemoattractant for T cells (Zhai et al., 2008; Sankar et al., 2006), as well as directs the expression of factors

that regulate ubiquitination (Maelfait and Beyaert, 2012) and a variety of cell signaling process (Zhou et al., 2017). Thus we propose that IRF3-target genes include a variety of anti-cccDNA effectors in addition to the known actions of the APOBEC genes. These effector genes then impart pleiotropic actions to (1) suppress cccDNA amplification, (2) destabilize cccDNA and/or enhance cccDNA degradation, (3) impact nuclear translocation or control uncoating/disassembly of the nucleocapsid to release RC DNA for cccDNA formation (Kock et al., 2003; Rabe et al., 2003; Cui et al., 2015), and (4) regulate the extrachromosomal DNA metabolism to impact HBV cccDNA formation (Luo et al., 2020; Blackford and Jackson, 2017). Indeed, we observed a marked reduction in the cccDNA $t_{1/2}$ when cells were treated with F7 or poly-U/UC PAMP, and this reduction was further enhanced when cells were co-treated with either of these plus ETV. In addition, for poly-U/UC PAMP, the antiviral actions against cccDNA could also include IFN-mediated actions directed by the low-level IFN induction (Lucifora et al., 2014; Phillips et al., 2017; Xu et al., 2018; Robek et al., 2005; Isorce et al., 2016). Interestingly, these actions of IFN and specific ISGs resulting from treatment with poly-U/UC PAMP could have contributed to a suppression of cccDNA resulting in a modestly shorter half-life compared with treatment with F7. How RIG-I/IRF3 signaling activation triggers cccDNA destabilization or degradation remains to be determined. The antiviral action of F7 and poly-U/UC PAMP might also include regulation of extrachromosomal DNA metabolism in addition to function of cytidine deaminases such as APOBEC3 genes. As HBV takes advantage of host DNA repair factors to repair the discontinuity of RC-DNA and convert it into a transcription permissive cccDNA, one or more of these steps of cccDNA production and maintenance could possibly be impacted by RIG-I/IRF3 actions (Long et al., 2017) (Sheraz et al., 2019) (Luo et al., 2020) (Qi et al., 2016; Tang et al., 2019).

Our studies demonstrated that we can specifically target RIG-I and IRF3 to activate the RLR innate immune program for the control of HBV infection through suppression of cccDNA, reducing the $t_{1/2}$ to days compared with weeks or months in the absence of treatment. Targeting innate immunity and the RLR pathway thus offers an effective strategy toward the design of new antiviral therapies against HBV that can be offered alone or in combination with NA for HBV treatment. Determining the innate immune targets directed by RIG-I and IRF3 that impart depletion of cccDNA will bring insight into the mechanism of action and unique antiviral properties of these unique drug candidates toward an HBV cure.

Limitations of the study

Our data indicate that administration of RIG-I agonists do not confer cytotoxicity using cellular ATP measurement methods. However, the potential cellular toxicity of innate immune modulation is yet to be evaluated *in vivo*. The biological actions of our RIG-I agonists are currently being examined in animal models.

Resource availability

Lead contact

Further information and requests for resources and reagents should be directed to and will be fulfilled by the corresponding author, Dr. Michael Gale, Jr. (mgale@uw.edu).

Materials availability

The F7 small molecule and poly-U/UC RNA production template are available from the corresponding author upon reasonable request.

Data and code availability

This study did not generate/analyze datasets and code.

Methods

All methods can be found in the accompanying Transparent methods supplemental file.

Supplemental information

Supplemental information can be found online at https://doi.org/10.1016/j.isci.2020.101969.

Acknowledgments

We are most grateful to Dr. Ju-Tao Guo (Baruch S. Blumberg Institute), Dr. Aleem Siddiqui (University of California San Diego), and Dr. T. Jake Liang (National Institutes of Health) for HepG2-hNTCP, HepAD38, and HepaRG cell lines.

This study was supported by National Institutes of Health (NIH) grants AI127463 and AI118916, and by NIH contracts HHSN272201300023C, 75N93019C00043, and HHSN272201400055C (M.G.). Portions on this work were also done under the auspices of the U.S. Dept. of Energy under contract 89233218CNA000001 and additionally supported by NIH grants AI078881, AI116868 and OD011095 (A.S.P.).

Author contributions

S.L. and M.G. designed the experiments and interpreted the results. S.L. performed experiments and statistical analysis. A.G. and A.S.P. analyzed the cccDNA half-life using a mathematical model. Y.I. and T.S. performed isolation and culture of primary human hepatocytes. S.L. and M.G. wrote the manuscript with input from all authors.

Declaration of interests

None to report. The authors declare no competing interests.

Received: July 10, 2020
Revised: October 29, 2020
Accepted: December 16, 2020
Published: January 22, 2021

References

Beck, J., and Nassal, M. (2007). Hepatitis B virus replication. World J. Gastroenterol. *13*, 48–64.

Bedard, K.M., Wang, M.L., Proll, S.C., Loo, Y.M., Katze, M.G., Gale, M., Jr., and Iadonato, S.P. (2012). Isoflavone agonists of IRF-3 dependent signaling have antiviral activity against RNA viruses. J. Virol. *86*, 7334–7344.

Belloni, L., Allweiss, L., Guerrieri, F., Pediconi, N., Volz, T., Pollicino, T., Petersen, J., Raimondo, G., Dandri, M., and Levrero, M. (2012). IFN-alpha inhibits HBV transcription and replication in cell culture and in humanized mice by targeting the epigenetic regulation of the nuclear cccDNA minichromosome. J. Clin. Invest. *122*, 529–537.

Blackford, A.N., and Jackson, S.P. (2017). ATM, ATR, and DNA-PK: the trinity at the heart of the DNA damage response. Mol. Cell *66*, 801–817.

Boni, C., Vecchi, A., Rossi, M., Laccabue, D., Giuberti, T., Alfieri, A., Lampertico, P., Grossi, G., Facchetti, F., Brunetto, M.R., et al. (2018). TLR7 agonist increases responses of hepatitis B virus-specific T cells and natural killer cells in patients with chronic hepatitis B treated with nucleos(T)ide analogues. Gastroenterology *154*, 1764–1777.e7.

Bonvin, M., Achermann, F., Greeve, I., Stroka, D., Keogh, A., Inderbitzin, D., Candinas, D., Sommer, P., Wain-Hobson, S., Vartanian, J.P., and Greeve, J. (2006). Interferon-inducible expression of APOBEC3 editing enzymes in human hepatocytes and inhibition of hepatitis B virus replication. Hepatology *43*, 1364–1374.

Chang, J., Block, T.M., and Guo, J.T. (2012). The innate immune response to hepatitis B virus infection: implications for pathogenesis and therapy. Antivir. Res. *96*, 405–413.

Chen, Z., Zhu, M., Pan, X., Zhu, Y., Yan, H., Jiang, T., Shen, Y., Dong, X., Zheng, N., Lu, J., et al. (2014). Inhibition of Hepatitis B virus replication by SAMHD1. Biochem. Biophys. Res. Commun. *450*, 1462–1468.

Chow, K.T., Gale, M., Jr., and Loo, Y.M. (2018). RIG-I and other RNA sensors in antiviral immunity. Annu. Rev. Immunol. *36*, 667–694.

Cui, X., Luckenbaugh, L., Bruss, V., and Hu, J. (2015). Alteration of mature nucleocapsid and enhancement of covalently closed circular DNA formation by hepatitis B virus core mutants defective in complete-virion formation. J. Virol. *89*, 10064–10072.

Dassler-Plenker, J., Paschen, A., Putschli, B., Rattay, S., Schmitz, S., Goldeck, M., Bartok, E., Hartmann, G., and Coch, C. (2019). Direct RIG-I activation in human NK cells induces TRAIL-dependent cytotoxicity toward autologous melanoma cells. Int. J. Cancer *144*, 1645–1656.

Dienstag, J.L. (2009). Benefits and risks of nucleoside analog therapy for hepatitis B. Hepatology *49*, S112–S121.

Fanning, G.C., Zoulim, F., Hou, J., and Bertoletti, A. (2019). Therapeutic strategies for hepatitis B virus infection: towards a cure. Nat. Rev. Drug Discov. *19*, 291.

Fensterl, V., and Sen, G.C. (2011). The ISG56/IFIT1 gene family. J. Interferon Cytokine Res. *31*, 71–78.

Fensterl, V., and Sen, G.C. (2015). Interferon-induced Ifit proteins: their role in viral pathogenesis. J. Virol. *89*, 2462–2468.

Fernandes-Alnemri, T., Yu, J.W., Datta, P., Wu, J., and Alnemri, E.S. (2009). AIM2 activates the inflammasome and cell death in response to cytoplasmic DNA. Nature *458*, 509–513.

Gish, R., Jia, J.D., Locarnini, S., and Zoulim, F. (2012). Selection of chronic hepatitis B therapy with high barrier to resistance. Lancet Infect. Dis. *12*, 341–353.

Guo, H., Jiang, D., Zhou, T., Cuconati, A., Block, T.M., and Guo, J.-T. (2007). Characterization of the intracellular deproteinized relaxed circular DNA of hepatitis B virus: an intermediate of covalently closed circular DNA formation. J. Virol. *81*, 12472–12484.

Han, Q., Hou, Z., Yin, C., Zhang, C., and Zhang, J. (2019). 5′-triphosphate siRNA targeting HBx elicits a potent anti-HBV immune response in pAAV-HBV transfected mice. Antiviral Res *161*, 36–45.

Hirt, B. (1967). Selective extraction of polyoma DNA from infected mouse cell cultures. J. Mol. Biol. *26*, 365–369.

Hochheiser, K., Klein, M., Gottschalk, C., Hoss, F., Scheu, S., Coch, C., Hartmann, G., and Kurts, C. (2016). Cutting edge: the RIG-I ligand 3pRNA potently improves CTL cross-priming and facilitates antiviral vaccination. J. Immunol. *196*, 2439–2443.

Horner, S.M., and Gale, M., Jr. (2013). Regulation of hepatic innate immunity by hepatitis C virus. Nat. Med. *19*, 879–888.

Huang, Q., Zhou, B., Cai, D., Zong, Y., Wu, Y., Liu, S., Mercier, A., Guo, H., Hou, J., Colonno, R., and Sun, J. (2020). Rapid turnover of HBV cccDNA indicated by monitoring emergence and reversion of signature-mutation in treated chronic hepatitis B patients. Hepatology. https://doi.org/10.1002/hep.31240.

Iadonato, S.P., Kaiser, S., Bedard, K.M., Fowler, K.W., and Madu, I. (2018). Anti-viral Compounds, Pharmaceutical Compositions, and Methods of Use Thereof (United States Patent Office: US patent 9,884,876 B2), pp. 23–24.

Isorce, N., Testoni, B., Locatelli, M., Fresquet, J., Rivoire, M., Luangsay, S., Zoulim, F., and Durantel, D. (2016). Antiviral activity of various interferons and pro-inflammatory cytokines in non-transformed cultured hepatocytes infected with hepatitis B virus. Antiviral Res *130*, 36–45.

Janssen, H.L., Van Zonneveld, M., Senturk, H., Zeuzem, S., Akarca, U.S., Cakaloglu, Y., Simon, C., So, T.M., Gerken, G., De Man, R.A., et al. (2005). Pegylated interferon alfa-2b alone or in combination with lamivudine for HBeAg-positive chronic hepatitis B: a randomised trial. Lancet *365*, 123–129.

Jefferies, M., Rauff, B., Rashid, H., Lam, T., and Rafiq, S. (2018). Update on global epidemiology of viral hepatitis and preventive strategies. World J. Clin. Cases *6*, 589–599.

Kell, A., Stoddard, M., Li, H., Marcotrigiano, J., Shaw, G.M., and Gale, M., Jr. (2015). Pathogen-associated molecular pattern recognition of hepatitis C virus transmitted/founder variants by RIG-I is dependent on U-core length. J. Virol. *89*, 11056–11068.

Ko, C., Chakraborty, A., Chou, W.M., Hasreiter, J., Wettengel, J.M., Stadler, D., Bester, R., Asen, T., Zhang, K., Wisskirchen, K., et al. (2018). Hepatitis B virus genome recycling and de novo secondary infection events maintain stable cccDNA levels. J. Hepatol. *69*, 1231–1241.

Kock, J., Kann, M., Putz, G., Blum, H.E., and Von Weizsacker, F. (2003). Central role of a serine phosphorylation site within duck hepatitis B virus core protein for capsid trafficking and genome release. J. Biol. Chem. *278*, 28123–28129.

Kwon, H., and Lok, A.S. (2011). Hepatitis B therapy. Nat. Rev. Gastroenterol. Hepatol. *8*, 275–284.

Lanford, R.E., Guerra, B., Chavez, D., Giavedoni, L., Hodara, V.L., Brasky, K.M., Fosdick, A., Frey, C.R., Zheng, J., Wolfgang, G., et al. (2013). GS-9620, an oral agonist of Toll-like receptor-7, induces prolonged suppression of hepatitis B virus in chronically infected chimpanzees. Gastroenterology *144*, 1508–1517.

Langley, D.R., Walsh, A.W., Baldick, C.J., Eggers, B.J., Rose, R.E., Levine, S.M., Kapur, A.J., Colonno, R.J., and Tenney, D.J. (2007). Inhibition of hepatitis B virus polymerase by entecavir. J. Virol. *81*, 3992–4001.

Lee, J.H., Chiang, C., and Gack, M.U. (2019). Endogenous nucleic acid recognition by RIG-I-like receptors and cGAS. J. Interferon Cytokine Res. *39*, 450–458.

Liang, T.J., Block, T.M., Mcmahon, B.J., Ghany, M.G., Urban, S., Guo, J.T., Locarnini, S., Zoulim, F., Chang, K.M., and Lok, A.S. (2015). Present and future therapies of hepatitis B: from discovery to cure. Hepatology *62*, 1893–1908.

Locarnini, S., Hatzakis, A., Chen, D.S., and Lok, A. (2015). Strategies to control hepatitis B: public policy, epidemiology, vaccine and drugs. J. Hepatol. *62*, S76–S86.

Long, Q., Yan, R., Hu, J., Cai, D., Mitra, B., Kim, E.S., Marchetti, A., Zhang, H., Wang, S., Liu, Y., et al. (2017). The role of host DNA ligases in hepadnavirus covalently closed circular DNA formation. PLoS Pathog. *13*, e1006784.

Lucifora, J., Xia, Y., Reisinger, F., Zhang, K., Stadler, D., Cheng, X., Sprinzl, M.F., Koppensteiner, H., Makowska, Z., Volz, T., et al. (2014). Specific and nonhepatotoxic degradation of nuclear hepatitis B virus cccDNA. Science *343*, 1221–1228.

Luo, J., Luckenbaugh, L., Hu, H., Yan, Z., Gao, L., and Hu, J. (2020). Involvement of host ATR-CHK1 pathway in hepatitis B virus covalently closed circular DNA formation. mBio *11*, e03423-19.

Maelfait, J., and Beyaert, R. (2012). Emerging role of ubiquitination in antiviral RIG-I signaling. Microbiol. Mol. Biol. Rev. *76*, 33–45.

Marion, P.L., and Robinson, W.S. (1983). Hepadna viruses: hepatitis B and related viruses. Curr. Top. Microbiol. Immunol. *105*, 99–121.

Maynard, M., Parvaz, P., Durantel, S., Chevallier, M., Chevallier, P., Lot, M., Trepo, C., and Zoulim, F. (2005). Sustained HBs seroconversion during lamivudine and adefovir dipivoxil combination therapy for lamivudine failure. J. Hepatol. *42*, 279–281.

Moucari, R., Korevaar, A., Lada, O., Martinot-Peignoux, M., Boyer, N., Mackiewicz, V., Dauvergne, A., Cardoso, A.C., Asselah, T., Nicolas-Chanoine, M.H., et al. (2009). High rates of HBsAg seroconversion in HBeAg-positive chronic hepatitis B patients responding to interferon: a long-term follow-up study. J. Hepatol. *50*, 1084–1092.

Mutz, P., Metz, P., Lempp, F.A., Bender, S., Qu, B., Schoneweis, K., Seitz, S., Tu, T., Restuccia, A., Frankish, J., et al. (2018). HBV bypasses the innate immune response and does not protect HCV from antiviral activity of interferon. Gastroenterology *154*, 1791–1804.e22.

Nassal, M. (2015). HBV cccDNA: viral persistence reservoir and key obstacle for a cure of chronic hepatitis B. Gut *64*, 1972–1984.

Newbold, J.E., Xin, H., Tencza, M., Sherman, G., Dean, J., Bowden, S., and Locarnini, S. (1995). The covalently closed duplex form of the hepadnavirus genome exists in situ as a heterogeneous population of viral minichromosomes. J. Virol. *69*, 3350–3357.

Ott, J.J., Stevens, G.A., Groeger, J., and Wiersma, S.T. (2012). Global epidemiology of hepatitis B virus infection: new estimates of age-specific HBsAg seroprevalence and endemicity. Vaccine *30*, 2212–2219.

Pandey, S., Kawai, T., and Akira, S. (2014). Microbial sensing by Toll-like receptors and intracellular nucleic acid sensors. Cold Spring Harb. Perspect. Biol. *7*, a016246.

Pattabhi, S., Wilkins, C.R., Dong, R., Knoll, M.L., Posakony, J., Kaiser, S., Mire, C.E., Wang, M.L., Ireton, R.C., Geisbert, T.W., et al. (2016). Targeting innate immunity for antiviral therapy through small molecule agonists of the RLR pathway. J. Virol. *90*, 2372–2387.

Perrillo, R. (2009). Benefits and risks of interferon therapy for hepatitis B. Hepatology *49*, S103–S111.

Phillips, S., Mistry, S., Riva, A., Cooksley, H., Hadzhiolova-Lebeau, T., Plavova, S., Katzarov, K., Simonova, M., Zeuzem, S., Woffendin, C., et al. (2017). Peg-interferon lambda treatment induces robust innate and adaptive immunity in chronic hepatitis B patients. Front. Immunol. *8*, 621.

Probst, P., Grigg, J.B., Wang, M., Munoz, E., Loo, Y.M., Ireton, R.C., Gale, M., Jr., Iadonato, S.P., and Bedard, K.M. (2017). A small-molecule IRF3 agonist functions as an influenza vaccine adjuvant by modulating the antiviral immune response. Vaccine *35*, 1964–1971.

Qi, Y., Gao, Z., Xu, G., Peng, B., Liu, C., Yan, H., Yao, Q., Sun, G., Liu, Y., Tang, D., et al. (2016). DNA polymerase kappa is a key cellular factor for the formation of covalently closed circular DNA of hepatitis B virus. PLoS Pathog. *12*, e1005893.

Rabe, B., Vlachou, A., Panté, N., Helenius, A., and Kann, M. (2003). Nuclear import of hepatitis B virus capsids and release of the viral genome. Proc. Natl. Acad. Sci. U S A *100*, 9849–9854.

Robek, M.D., Boyd, B.S., and Chisari, F.V. (2005). Lambda interferon inhibits hepatitis B and C virus replication. J. Virol. *79*, 3851–3854.

Saito, T., Owen, D.M., Jiang, F., Marcotrigiano, J., and Gale, M., Jr. (2008). Innate immunity induced by composition-dependent RIG-I recognition of hepatitis C virus RNA. Nature *454*, 523–527.

Sankar, S., Chan, H., Romanow, W.J., Li, J., and Bates, R.J. (2006). IKK-i signals through IRF3 and NFkappaB to mediate the production of inflammatory cytokines. Cell. Signal. *18*, 982–993.

Schnell, G., Loo, Y.M., Marcotrigiano, J., and Gale, M., Jr. (2012). Uridine composition of the poly-U/UC tract of HCV RNA defines non-self recognition by RIG-I. PLoS Pathog. *8*, e1002839.

Seeger, C., and Mason, W.S. (2000). Hepatitis B virus biology. Microbiol. Mol. Biol. Rev. *64*, 51–68.

Sheraz, M., Cheng, J., Tang, L., Chang, J., and Guo, J.T. (2019). Cellular DNA topoisomerases are required for the synthesis of hepatitis B virus covalently closed circular DNA. J. Virol. *93*, e02230-18.

Shi, L., Li, S., Shen, F., Li, H., Qian, S., Lee, D.H., Wu, J.Z., and Yang, W. (2012). Characterization of nucleosome positioning in hepadnaviral covalently closed circular DNA minichromosomes. J. Virol. *86*, 10059–10069.

Tang, L., Sheraz, M., Mcgrane, M., Chang, J., and Guo, J.T. (2019). DNA Polymerase alpha is essential for intracellular amplification of hepatitis

B virus covalently closed circular DNA. PLoS Pathog. *15*, e1007742.

Tang, L., Zhao, Q., Wu, S., Cheng, J., Chang, J., and Guo, J.T. (2017). The current status and future directions of hepatitis B antiviral drug discovery. Expert Opin. Drug Discov. *12*, 5–15.

Turelli, P., Mangeat, B., Jost, S., Vianin, S., and Trono, D. (2004). Inhibition of hepatitis B virus replication by APOBEC3G. Science *303*, 1829.

Tuttleman, J.S., Pourcel, C., and Summers, J. (1986). Formation of the pool of covalently closed circular viral DNA in hepadnavirus-infected cells. Cell *47*, 451–460.

Unterholzner, L., Keating, S.E., Baran, M., Horan, K.A., Jensen, S.B., Sharma, S., Sirois, C.M., Jin, T., Latz, E., Xiao, T.S., et al. (2010). IFI16 is an innate immune sensor for intracellular DNA. Nat. Immunol. *11*, 997–1004.

Wang, G.H., and Seeger, C. (1993). Novel mechanism for reverse transcription in hepatitis B viruses. J. Virol. *67*, 6507–6512.

Watashi, K., Sluder, A., Daito, T., Matsunaga, S., Ryo, A., Nagamori, S., Iwamoto, M., Nakajima, S., Tsukuda, S., Borroto-Esoda, K., et al. (2014). Cyclosporin A and its analogs inhibit hepatitis B virus entry into cultured hepatocytes through targeting a membrane transporter, sodium taurocholate cotransporting polypeptide (NTCP). Hepatology *59*, 1726–1737.

Werle-Lapostolle, B., Bowden, S., Locarnini, S., Wursthorn, K., Petersen, J., Lau, G., Trepo, C., Marcellin, P., Goodman, Z., Delaney, W.E.T., et al. (2004). Persistence of cccDNA during the natural history of chronic hepatitis B and decline during adefovir dipivoxil therapy. Gastroenterology *126*, 1750–1758.

Wieland, S., Thimme, R., Purcell, R.H., and Chisari, F.V. (2004). Genomic analysis of the host response to hepatitis B virus infection. Proc. Natl. Acad. Sci. U S A *101*, 6669–6674.

Wu, S., Lin, J., Fu, Y., and Ou, Q. (2018). RIG-I enhances interferon-alpha response by promoting antiviral protein expression in patients with chronic hepatitis B. Antivir. Ther. *23*, 575–583.

Wu, T.T., Coates, L., Aldrich, C.E., Summers, J., and Mason, W.S. (1990). In hepatocytes infected with duck hepatitis B virus, the template for viral RNA synthesis is amplified by an intracellular pathway. Virology *175*, 255–261.

Wursthorn, K., Lutgehetmann, M., Dandri, M., Volz, T., Buggisch, P., Zollner, B., Longerich, T., Schirmacher, P., Metzler, F., Zankel, M., et al. (2006). Peginterferon alpha-2b plus adefovir induce strong cccDNA decline and HBsAg reduction in patients with chronic hepatitis B. Hepatology *44*, 675–684.

Xia, Y., Stadler, D., Lucifora, J., Reisinger, F., Webb, D., Hosel, M., Michler, T., Wisskirchen, K., Cheng, X., Zhang, K., et al. (2016). Interferon-gamma and tumor necrosis factor-alpha produced by T cells reduce the HBV persistence form, cccDNA, without cytolysis. Gastroenterology *150*, 194–205.

Xu, F., Song, H., Xiao, Q., Li, N., Zhang, H., Cheng, G., and Tan, G. (2018). Type III interferon-induced CBFβ inhibits HBV replication by hijacking HBx. Cell Mol. Immunol. *16*, 357–366.

Yan, H., Zhong, G., Xu, G., He, W., Jing, Z., Gao, Z., Huang, Y., Qi, Y., Peng, B., Wang, H., et al. (2012). Sodium taurocholate cotransporting polypeptide is a functional receptor for human hepatitis B and D virus. Elife *1*, e00049.

Zhai, Y., Shen, X.D., Gao, F., Zhao, A., Freitas, M.C., Lassman, C., Luster, A.D., Busuttil, R.W., and Kupiec-Weglinski, J.W. (2008). CXCL10 regulates liver innate immune response against ischemia and reperfusion injury. Hepatology *47*, 207–214.

Zhou, Y., He, C., Wang, L., and Ge, B. (2017). Post-translational regulation of antiviral innate signaling. Eur. J. Immunol. *47*, 1414–1426.

Zoulim, F., and Durantel, D. (2015). Antiviral therapies and prospects for a cure of chronic hepatitis B. Cold Spring Harb. Perspect. Med. *5*, a021501.

Zoulim, F., and Locarnini, S. (2009). Hepatitis B virus resistance to nucleos(t)ide analogues. Gastroenterology *137*, 1593–1608.e1-2.

iScience, Volume *24*

Supplemental Information

Suppression of hepatitis B virus through therapeutic activation of RIG-I and IRF3 signaling in hepatocytes

Sooyoung Lee, Ashish Goyal, Alan S. Perelson, Yuji Ishida, Takeshi Saito, and Michael Gale Jr.

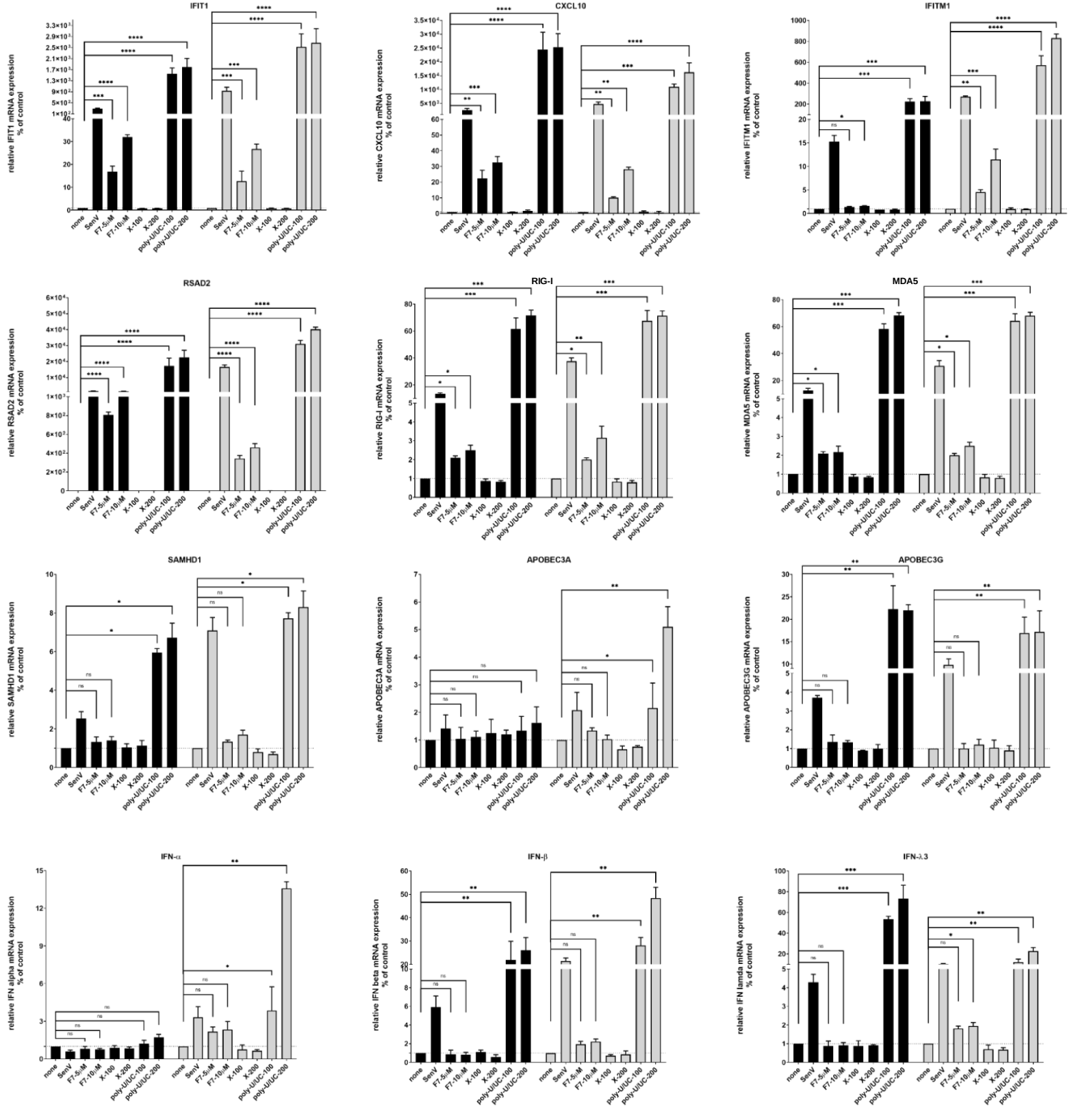
IFIT1
relative IFIT1 mRNA expression % of control
CXCL10
relative CXCL10 mRNA expression % of control
IFITM1
relative IFITM1 mRNA expression % of control
RSAD2
relative RSAD2 mRNA expression % of control
RIG-I
relative RIG-I mRNA expression % of control
MDA5
relative MDA5 mRNA expression % of control
SAMHD1
relative SAMHD1 mRNA expression % of control
APOBEC3A
relative APOBEC3A mRNA expression % of control
APOBEC3G
relative APOBEC3G mRNA expression % of control
IFN-α
relative IFN alpha mRNA expression % of control
IFN-β
relative IFN beta mRNA expression % of control
IFN-λ3
relative IFN lamda mRNA expression % of control
none
SenV
F7-5i;M
F7-10i;M
X-100
X-200
poly-U/UC-100
poly-U/UC-200
24 hours post treatment
72 hours post treatment

Figure S1. F7 and poly-U/UC induce differential innate immune genes expression, Related to Figure 1. HepG2-hNTCP cells were infected with SenV (positive control) or treated with F7 (5 or 10 uM as indicated), X-RNA (100 ng/ml; X-100 and 200 ng/ml; X-200) or poly-U/UC PAMP 100 ng/ml or 200ng/ml as indicated for 24 and 72 hours. Cells were harvested at each time point. Total cellular RNA was purified and subjected to RT-qPCR analysis to measure the expression level of a panel of innate immune genes including IFIT1, CXCL10, IFITM1, RSAD2, RIG-I, MDA5, SAMHD1, APOBEC3A, APOBEC3G, IFN-α, IFN-β, and IFN-λ3. Gene expression levels were normalized to the level of GAPDH expression in each sample, and are expressed as the fold induction over that achieved with 2.5 % DMSO treatment (negative control) from three independent experiments. Data was presented as mean ± standard deviation (SD), * $P < 0.01$, ** $P < 0.005$, *** $P < 0.0005$, **** $P < 0.0001$, and ns=non-significant.

A

F7

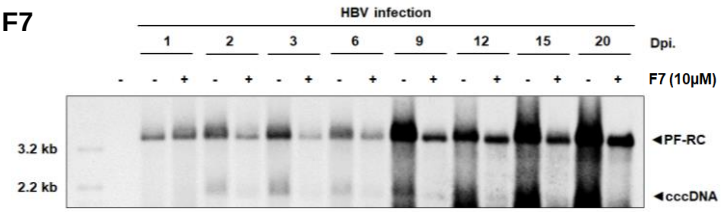

Poly-U/UC PAMP

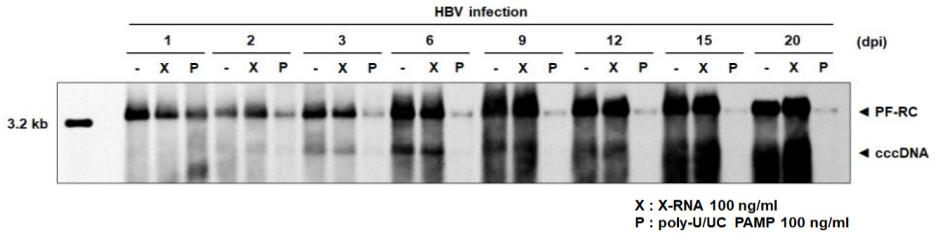

X : X-RNA 100 ng/ml
P : poly-U/UC PAMP 100 ng/ml

B

F7

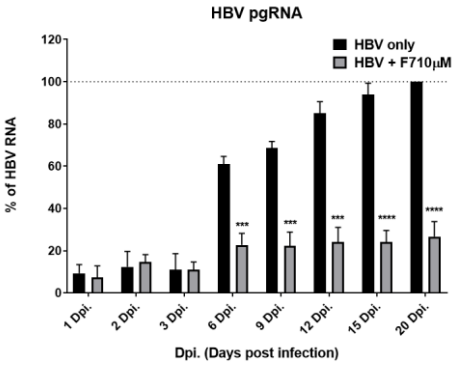

Poly-U/UC PAMP

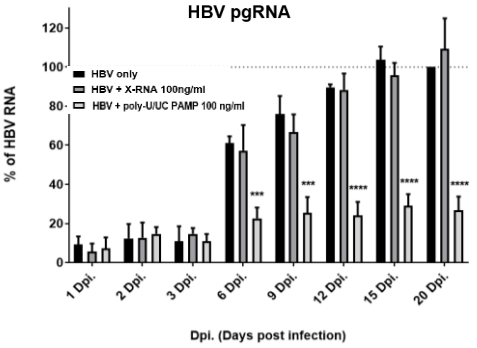

C

F7

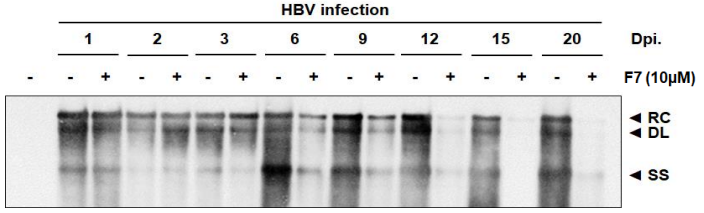

Poly-U/UC PAMP

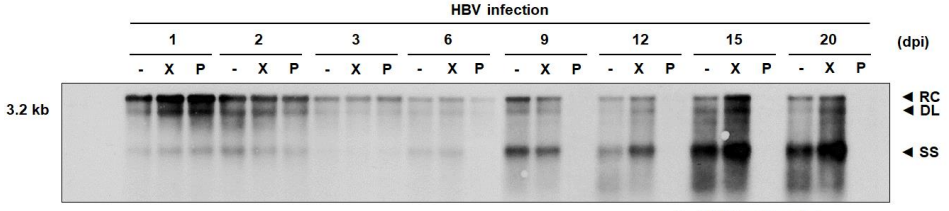

X : X-RNA 100 ng/ml
P : poly-U/UC PAMP 100 ng/ml

D

F7

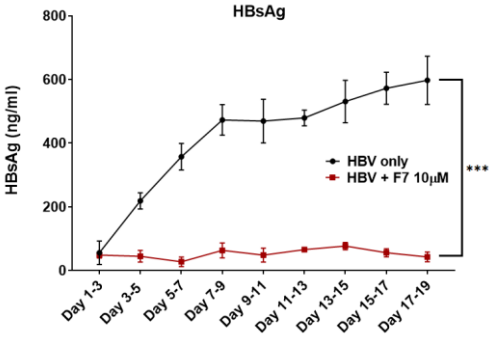

E

F7

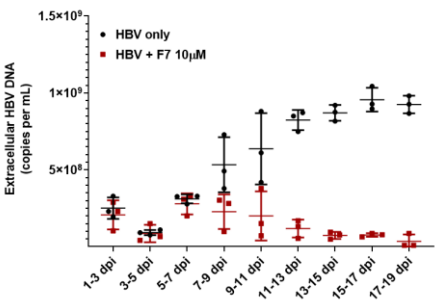

Poly-U/UC PAMP

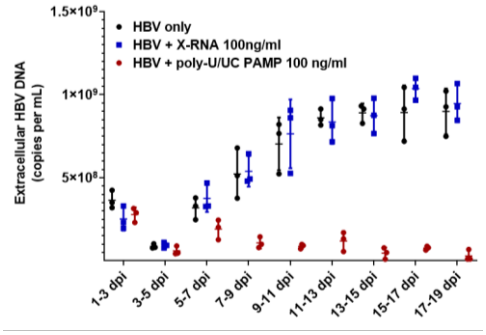

Poly-U/UC PAMP HBsAg

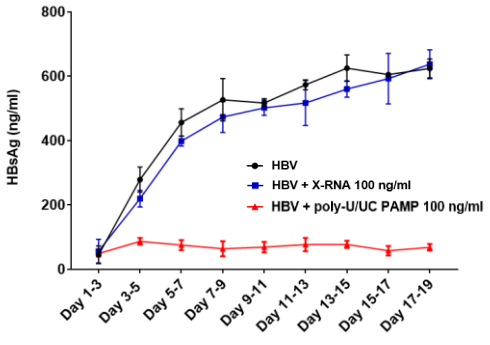

Figure S2. Kinetics of HBV replication in parallel cultures of cells during treatment with F7 or poly-U/UC PAMP, Related to Figure 2. HepG2-hNTCP cells were infected with HBV at a moi of 1000 Geq/cell. After 24 hr the cells were treated with F7 (10 μM) (upper), or 100 ng/ml X RNA or 100ng/ml poly-U/UC PAMP (lower). Cells were harvested at each time point, Hirt supernatants prepared and subjected to Southern blot analysis. (B) HBV pgRNA was analyzed by RT-qPCR. Values from 20 Dpi of 'HBV only' was set to 100% for RT-PCR analysis. Data was presented as mean ± standard deviations (SD), *** $P < 0.001$, **** $P < 0.0001$, and ns = non-significant.(C) HBV intracellular capsid-associated DNA from cells treated with 10 uM F7 (upper) or 100ng/ml XRNA or poly-U/UC PAMP (lower) was analyzed by Southern blot. (D) Secreted HBsAg from HBV-infected cells treated with F7 (upper) or poly-U/UC (lower) was detected by ELISA. (E) Extracellular HBV-DNA was measured by qPCR from cells treated with 10 uM (left) or 100 ng/ml XRNA or poly-U/UC PAMP (right). Data are presented as mean ± standard deviation (SD) from three independent experiments. *** $P = 0.0002$.

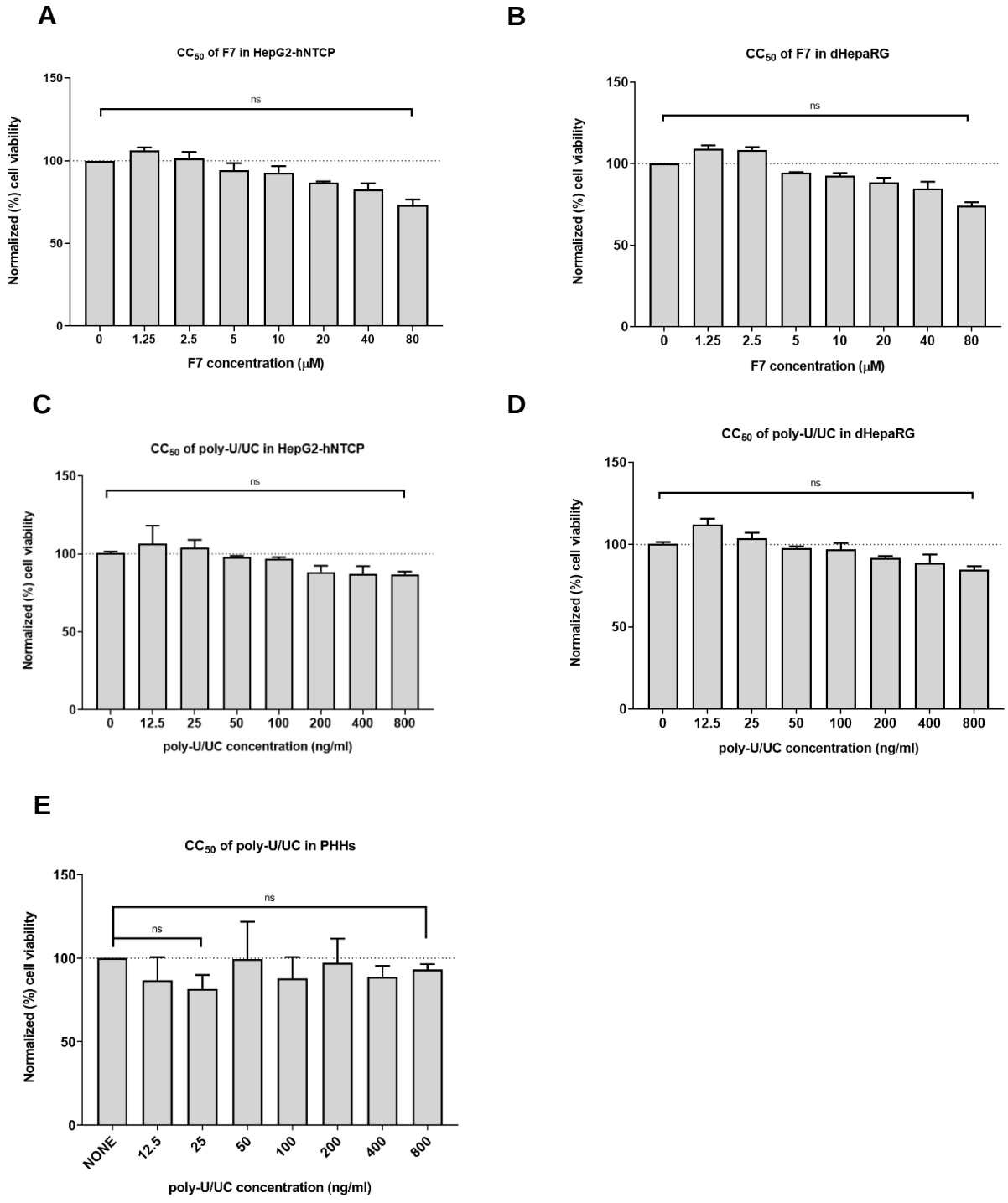

Figure S3. CC_{50} analysis of of F7 and poly-U/UC PAMP treatment, Related to Figure 3. HepG2-NTCP Cells (A and C), dHepaRG (B and D), and PHH (E) were treated with increasing doses of F7 or poly-U/UC PAMP for 72 hours. Cell viability was determined concurrently by measuring ATP content, with values normalized to mock-treated cells. Graph represents the mean of triplicated samples in each of 3 independent experiments, with error bars showing standard deviation. ns=non-significant.

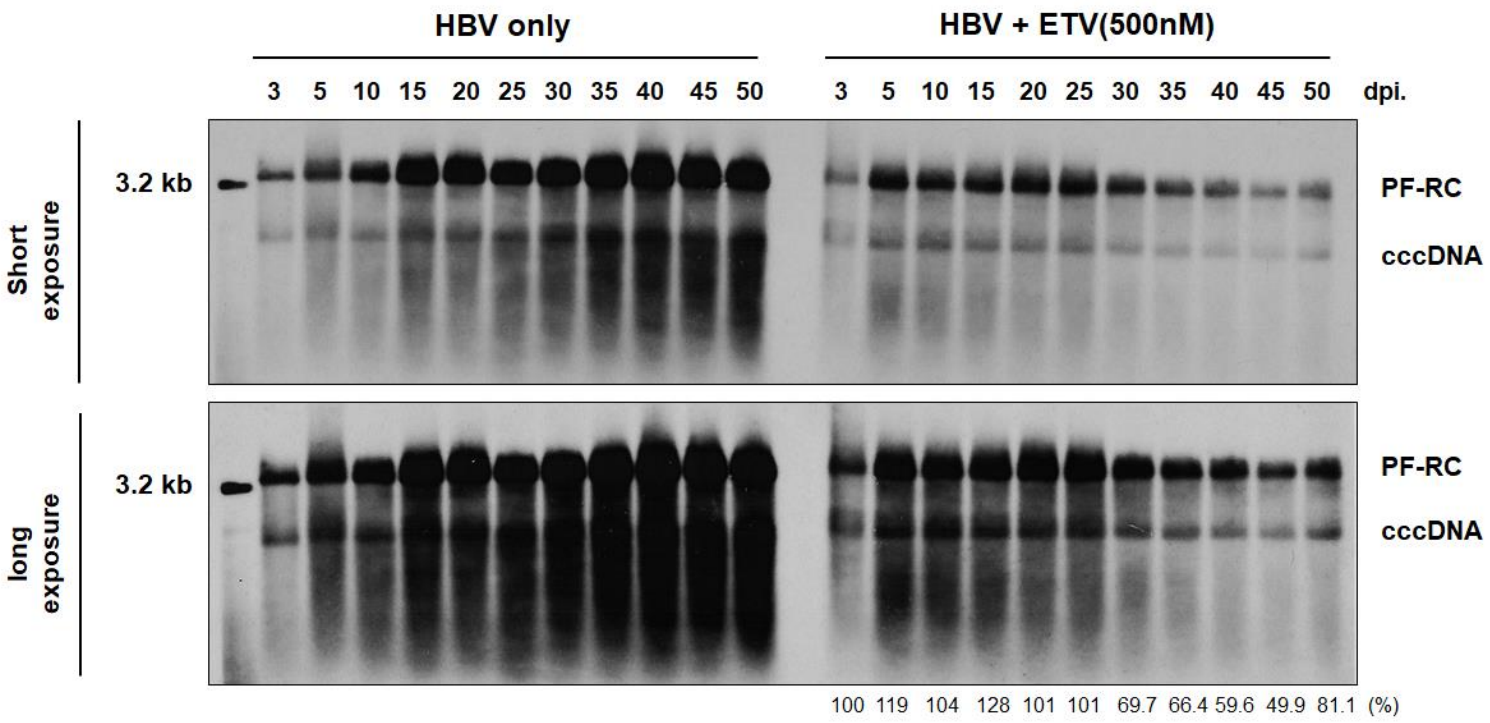

Figure S4. The half-life of cccDNA, Related to Figure 4. HepG2-NTCP cells were infected with HBV at an moi 1000 Geq/cell, At 3 dpi the cultures were left nontreated or were treated with ETV (500nM) through the full 50 day time course by replacing the media each day with fresh media alone or containing ETV. Cells were harvested at the indicated time points, DNA was isolated by Hirt extraction and analyzed by Southern blot using a HBV-specific probe. Percentage values below each lane indicate the relative amount of cccDNA present compared to day 3 levels.

Treatment	Parameter values	95% Confidence Interval
F7		
$t_{1/2}$ (days)	8.7	[7.2, 14.0]
τ (days)	4.0	[1.4, 6.6]
F7+ETV		
$t_{1/2}$ (days)	6.5	[5.5, 8.5]
τ (days)	3.7	[1.6, 5.8]
Poly-U/UC PAMP		
$t_{1/2}$ (days)	7.7	[7.4, 9.8]
τ (days)	3.8	[2.4, 5.2]
Poly-U/UC PAMP+ETV		
$t_{1/2}$ (days)	6.9	[5.8, 10.5]
τ (days)	2.6	[1.0, 4.3]

Figure S5. The half-life of cccDNA ($t_{1/2}$) and the delay before cccDNA starts decreasing (τ) estimated from the kinetics of decay of cccDNA under treatment, Related to Figure 5.

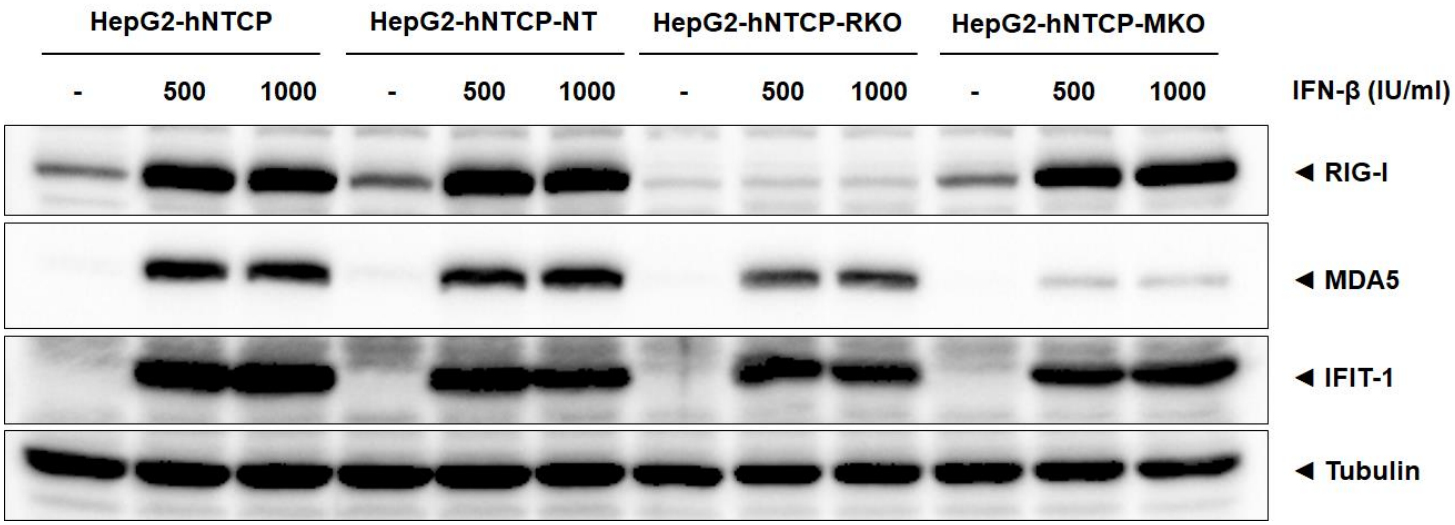

Figure S6. Immunoblot analysis of HepG2-hNTCP cells transduced with CRISPR/Cas9 guide RNA constructs to target RIG-I (RKO) or MDA5 (MKO) or nontargeteing guide RNA (NT) control, Related to Figure 6. Cells were treated with 100 U/ml IFN-b for 24 hrs. Cell lysates were prepared and analyze by immunoblot. The levels of RIG-I, MDA5, and IFIT1 and tubulin (house keeping protein control) were determined using respective antibodies.

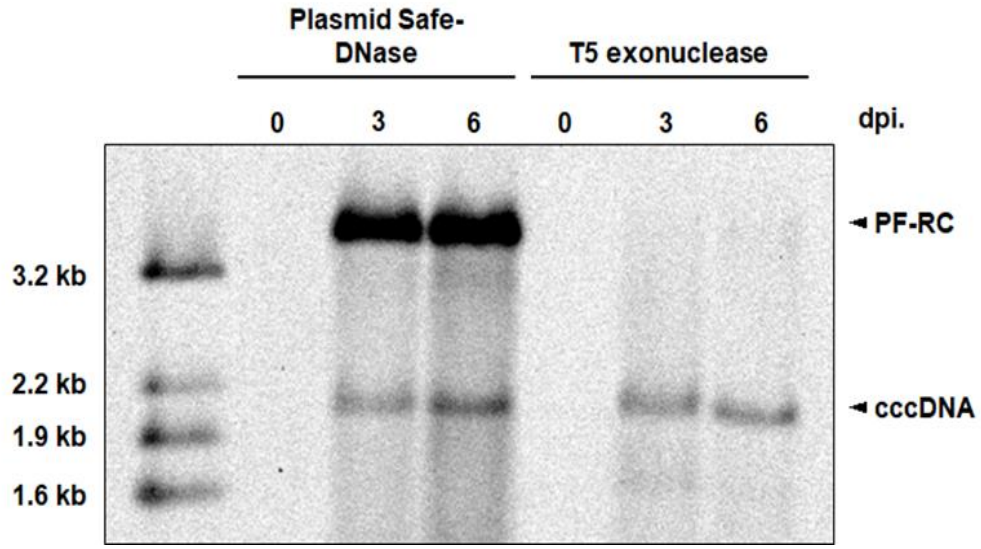

Figure S7. Southern blot analysis of protein-free HBV DNAs with plasmid safe-Dnase or T5 exonuclease treatment, Related to STAR Methods. HepG2-NTCP cells were infected with HBV at an moi 1000 Geq/cell. Cells were harvested at the indicated time points, DNA was isolated by Hirt extraction. Hirt-extracted protein free DNAs were treated with 10 units of Plasmid-safe DNase or 10 units of T5 exonuclease to digest different formed DNAs, and analyzed by Southern blot using a HBV-specific probe.

Table S1. Primer Sequences, Related to Methods

No	Oligoname	Sequence (5'→3')
1	HBV cccDNA Fwd	GCCTATTGATTGGAAAGTATGT
2	HBV cccDNA Rev	GCTGAGGCGGTATCTA
3	HBV pgRNA Fwd	CTCCTCCAGCTTATAGACC
4	HBV pgRNA Rev	GTGAGTGGGCCTACAAA
5	IFIT1 Fwd	AGAAGCAGGCAATCACAGAAAA
6	IFIT1 Rev	CTGAAACCGACCATAGTGGAAAT
7	IFITM1 Fwd	TACTCCGTGAAGTCTAGGGACAG
8	IFITM1 Rev	AACAGGATGAATCCAATGGTCA
9	CXCL10 Fwd	GTGGCATTCAAGGAGTACCTC
10	CXCL10 Rev	TGATGGCCTTCGATTCTGGATT
11	RSAD2 Fwd	CGTGAGCATCGTGAGCAATG
12	RSAD2 Rev	TCTTCTTTCCTTGGCCACGG
13	RIG-I Fwd	Qiagen SABiosciences # PPH20774A
14	RIG-I Rev	
15	MDA5 Fwd	Qiagen SABiosciences # PPH18927A
16	MDA5 Rev	
17	IFNα Fwd	TGCACCGAACTCTACCAGCA
18	IFNα Rev	GTTTCTCCCACCCTCTCCTCC
19	IFNβ Fwd	Qiagene SABiosciences # PPH00384F
20	IFNβ Rev	
21	IFNγ Fwd	Qiagene SABiosciences # PPH00380C
22	IFNγ Rev	
23	IFNλ3 Fwd	AAGGACTGCAAGTGCCGCT
24	IFNλ3 Rev	GCTGGTCCAAGACATCCC
25	SAMHD1 Fwd	TCACAGGCGCATTACTGCC
26	SAMHD1-Rev	GGATTTGAACCAATCGCTGGA
27	APOBEC3A Fwd	GAGAAGGGACAAGCACATGG
28	APOBEC3A Rev	TGGATCCATCAAGTGTCTGG
29	APOBEC3G Fwd	CCGAGGACCCGAAGGTTAC
30	APOBEC3G Rev	TCCAACAGTGCTGAAATTCG
31	GAPDH Fwd	ACAACTTTGGTATCGTGGAAGG
32	GAPDH Rev	GCCATCACGCCACAGTTTC
33	MT-CO3* Fwd	CCCCACAAACCCCATTACTAAACCCA
34	MT-CO3* Rev	TTTCATCATGCGGAGATGTTGGATGG

* MT-CO3 : mitochondrial cytochrome c oxidase subunit 3

Transparent Methods

Key Resources Table

REAGENT or RESOURCE	SOURCE	IDENTIFIER
Antibodies		
Rabbit anti-IRF3 phosphoserine 386	Cell Signaling	Cat#37829S
Rabbit anti-IRF3	Cell Signaling	Cat#4302S
Rabbit anti-IFIT1	This Study	
Rabbit anti-RIG-I	This Study	
Rabbit anti-MDA5	IBL	Cat#29020
Rabbit anti-Lamin B1	Abcam	Cat#ab16048
Mouse anti-Calnexin	Abcam	Cat#ab22595
Mouse anti-α-Tubulin	Cell Signaling	Cat#3873S
Bacterial and Virus Strains		
Sendai virus strain Cantell	Charles River Laboratory	Loo et al., 2008
Hepatitis B Virus Genotype D	HepAD38 cells	Ko et al., 2014a; Watashi et al., 2013
Chemicals, Peptides, and Recombinant Proteins		
Anti-Digoxigenin-AP Fab Fragments	Roche	Cat#16646821
Cell titer Glo Substrate	Promega	Cat#G755A
CSPD	Roche	Cat#70457821
Doxycycline Hyclate	Sigma	Cat#D9891
Entecavir	Sigma	Cat#SML1103
iScript select cDNA Synthesis Kit	Bio-Rad	Cat#1708897
MegaShortScript T7 High Yield Transcription Kit	Invitrogen	Cat#AM1354
PCR DIG Probe Synthesis Kit	Roche	Cat#11636090910
Phenol:Chloroform:Isoamyl alchol	Sigma	Cat#P2069
Plasmid-Safe ATP-dependent Dnase	Lucigen	Cat#E3101K
SYBR Green PCR master mix	Applied Biosystems	Cat#1906524
T5 exonuclease	NEB	Cat#M0363S
Critical Commercial Assays		

Quick Titer Hepatitis B Surface Antigen ELISA Kit	Cell Biolabs	Cat#VPK-5004
Experimental Models: Cell Lines		
Human: HepG2-C3A-hNTCP cells	provided by Dr. Ju-Tao Guo	Guo et al., 2017
Human: HepAD38 cells	provided by Dr. Aleem Siddiqui	Watashi et al., 2013
Human: HepaRG cells	provided by Dr. T. Jake Liang	Gripon et al., 2002
Human: PHH isolated from chimeric mice	This Study	Ishida et al., 2015
Oligonucleotides		
See Table S1 for primer sequences	N/A	N/A
Software and Algorithms		
Prism	GraphPad	http://www.graphpad.com/scientific-software/prism/
Fiji/Image J	Image J	http://fiji.sc/
Image Lab	Bio-Rad	http://www.bio-rad.com/en-uk/product/image-lad-software

Experimental model and subject details

Cell cultures: The human NTCP stably expressing human hepatoma cell line C3A, a subclone of HepG2 (kindly provided by Dr. Ju-Tao Guo, Baruch S. Blumberg Institute, USA) were maintained in Dulbecco modified Eagle medium (DMEM) supplemented with 10 % heat-inactivated FBS, 1 x Glutamax (GIBCO), 100 U/ml penicillin, and 100 µg/ml streptomycin and were selected/expanded with medium containing 1µg/ml of puromycin as previously described (Guo et al., 2017, Ko et al., 2014a). HepAD38 cell line, which support produce HBV in tetracycline (TET)-inducible manner, were maintained as previously described (kindly provided by Dr. Aleem Siddiqui, University of California San Diego, USA) (Watashi et al., 2013). The human liver progenitor HepaRG cell line was kindly provided by Dr. T. Jake Liang (National Institutes of Health, USA) and were cultured in complete William's E medium supplemented with 10% FBS, 100 U/ml penicillin, 100 µg/ml streptomycin,

Hydrocortisone 21-Hemisuccinate (Cayman), human insulin (Sigma), and 1 x Glutamax (GIBCO) (Gripon et al., 2002). Primary human hepatocytes were freshly isolated from chimeric mice that have humanized liver reconstituted with PHH. The recovered PHH were cultured in DMEM supplemented with 10% heat-inactivated FBS, 15μg/ml L-proline, 25ng/ml insulin, 50nM Dexamethasone, 5ng/ml EGF, and 0.1mM L-ascorbic acid 2-phospate, as described previously (Ishida et al., 2015).

Generation of HepG2-hNTCP-NT/ RIG-I / MDA5 KO cell lines by using CRISPR system: For expression of human sodium taurocholate co-transporting polypeptide (hNTCP), the gene coding sequence was amplified from a cDNA clone prepared from dHepaRG cells. A carboxyl-terminal C9 tag was added by PCR amplification. Transduced cells were selected with 20 μg/ml blasticidin and the best growing single cell clones were screened for their ability to support HBV infection. For CRISPR/Cas mediated gene knockout, guide RNA (gRNA) sequences were designed with the CRISPR tool of Benchling (Biology Software, 2017, https://benchling.com). The gRNA target oligonucleotides were cloned into Cas9-t2a-pRRL lentiviral vector by using the In-Fusion cloning kit (Takara). gRNA sequences used for gene knockouts were gRIG-I: 5'-GGGTCTTCCGGATATAATCC-3', and gMDA5: 5'-GTGGTTGGACTCGGGAATTCG-3' (Esser-Nobis et al., 2019). Upon transduction, cells were kept under continuous selection with 10 μg/ml puromycin and knockouts were confirmed by western blot.

Method details

HBV infection: HBV (Genotype D) was purified from the supernatant of HepAD38 cells by PEG concentration and subsequent sucrose gradient, as described previously (Watashi et al., 2013, Ko et al., 2014a). For HBV infection, cells were seeded into collagen-coated plates. One day later, the cells were infected with HBV in DMEM containing 4% polyethylene glycol 8000 (PEG-8000). The multiplicities of infection (expressed as virus genome equivalent/cell) are indicated in each Figure

Legend. The inocula were removed 24 hours later, and the infected cultures were maintained in complete DMEM containing 2.5% DMSO until harvesting, as described previously (Ni et al., 2014).

Reagents: F7 is a small molecule, N-(6-benzamido-1,3-benzothiazol-2-yl)naphthalene-2-carboxamide) (see Figure 1A), based on a benzothizol core structure identified in a high-throughput screen for IRF3 agonists(Probst et al., 2017, Iadonato et al., 2018). F7 structure was obtained from the published patent (Iadonato et al., 2018) and synthesized de novo by Medchem Source, Inc. for use in our studies. Sendai virus (SenV) strain Cantell was obtained from Charles River Laboratory, and working stocks were generated as previously described (Loo et al., 2008). Mirus Trans-IT mRNA transfection reagent was used treatment of cells with X-RNA and PAMP-RNA. Cyclosporin A (C1832) and Entecavir (SML1103) were obtained from Sigma Aldrich.

In vitro transcription: The poly-U/UC PAMP-RNA and X-RNA were each synthesized from T7 promoter-linked complementary oligonucleotides for the poly-U/UC PAMP RNA (Forward: 5′-TAATACGACTCACTATAGGCCATCCTGTTTTTTTCCCTTTTTTTTTTTCTTTTTTTTTTTTTTTTTTTTTTTTTTTTTTTTCTCCTTTTTTTTTCCTCTTTTTTTCCTTTTCTTTCCTTT-3′, Reverse: 5’-AAAGGAAAGAAAAGGAAAAAAAGAGGAAAAAAAAAGGAGAAAAAAAAAAAAAAAAAAAAAAAAAAAAAAAAAAAGGGAAAAAAACAGGATGGCCTATAGTGAGTCGTATTA -3’) and X-RNA (Forward: 5′-TAATACGACTCACTATAGGTGGCTCCATCTTAGCCCTAGTCACGGCTAGCTGTGAAAGGTCCGTGAGCCGCTTGACTGCAGAGAGTGCTGATACTGGCCTCTCTGCAGATCAAGT-3′, Reverse: 5’-ACTTGATCTGCAGAGAGGCCAGTATCAGCACTCTCTGCAGTCAAGCGGCTCACGGACCTTTCACAGCTAGCCGTGACTAGGGCTAAGATGGAGCCACCTATAGTGAGTCGTATTA -3’) as previously described (Saito et al., 2008, Kell et al., 2015). RNA products were generated by using T7 RNA polymerase and T7 MEGAshortscript kit (Ambion) according to the manufacturer's instructions. 10µg of oligonucleotide mixture were annealed using gradient PCR program (95°C 2min, with gradual temperature decrease by 1°C/30sec to 50°C). After annealing, the reaction mixture was assembled in an RNase-Free micro-centrifuge tube with 7.5mM of each nucleotide, 10x Reaction buffer, 2µg of template DNA and T7 enzyme as described by manufacturer, and the

reaction was incubated at 37°C for 4 hours to allow in vitro transcription. DNA templates were then removed with Turbo DNase treatment and unincorporated nucleotides and protein were removed by phenol-chloroform extraction. RNAs were precipitated by using ethanol and ammonium acetate as described by the manufacturer and resuspended in nuclease-free water. RNA concentrations were determined by absorbance using a Nanodrop spectrophotometer. RNA quality and purity were assessed on denaturing 2% formaldehyde agarose gels.

Reverse transcription quantitative real time PCR (RT-qPCR) and qPCR analyses: Total cellular RNAs were extracted from cells using TRIZOL reagent and the manufacturers' protocol (Invitrogen). cDNA was synthesized from the purified RNA by both random and oligo (dT) priming using iScript select cDNA synthesis kit (Biorad, Inc.). For HBV cccDNA expression analysis, total DNA was extracted using the DNeasy kit (QIAGEN). For selective cccDNA PCR analysis, isolated DNAs were treated with 10 units of T5 exonuclease (NEB) for 30 min 37°C and 5 min 95°C, and 4-fold dilution with Nuclease-free water. Phenol extraction was performed to remove any remaining T5 exonuclease prior to DNA analysis. Relative mRNA levels of all target genes were quantified by RT-qPCR performed using the ΔΔCT method, and expression levels were normalized to house-keeping genes. Real-time PCR assays were carried out using the SYBR green method (Applied Biosystems) performed using a Applied Biosystems 7300 thermocycler. Primer sequence information for RT-qPCR analysis of human and HBV genes is provided in Table S1.

Southern Blot analysis of HBV DNA: Southern blot analysis was performed on DNA isolated from cytoplasmic viral capsids exactly as previously described (Ko et al., 2014b, Ko et al., 2014a). To detect protein-free forms of HBV-DNA including cccDNA, a modified Hirt extraction method was used, as previously described (Guo et al., 2007, Cai et al., 2013). The Hirt extracted protein-free DNAs preparation was digested with plasmid-safe ATP-dependent DNase (Epicentre). The extracted Viral DNA forms were separated on 1.2 % agarose gel, transferred to positive charged nylon membrane (GE healthcare, Amersham) via upward capillary transfer, then hybridized with digoxigenin-labeled HBV-specific DNA probe. DNA signal was detected by DIG luminescent detection kit (Roche). To analyze protein-free forms of HBV DNAs, Hirt-extracted protein-free DNAs were treated with 10

units of Plasmid-safe DNase or 10 units of T5 exonuclease to digest the different forms of viral DNA. Southern blot analysis shows that while Plasmid Safe-DNAse treatment facilitated recovery of both PF-RC DNA and cccDNA, T5 exonuclease treatment resulted in recovery of cccDNA without detectable levels of PF-RC DNA (Figure S7). To assess DNA levels for equal loading of Southern blots, we performed qPCR to measure mitochondrial cytochrome c oxidase subunit 3(MT-CO3) levels in DNA preparations, which were then used to normalize DNA levels for equal gel/Southern blot loading.

Immunoblot analysis: Immunoblot analysis was performed essentially as described (Lee et al., 2016). Cells were lysed with RIPA buffer containing 0.1 % dodium dodecyl sulfate in the presence of protease and phosphatase inhibitor cocktail (Sigma Aldrich). Lysates were separated by SDS-PAGE followed by electrical transfer onto nitrocellulose membranes. The membranes were probed overnight at 4°C using the appropriate primary antibodies, and followed by the corresponding HRP-conjugated secondary antibodies. The following primary antibodies were used for this study: Rabbit anti-IRF3 phosphoserine 386 (Cell Signaling), Rabbit anti-IRF3 (Cell Signaling), Rabbit anti-IFIT1 (antibody 972; raised in rabbit against as IFIT1 437-490 aa peptide sequence), Rabbit anti-RIG-I (antibody 969; raised in rabbit against RIG-I aa 1-227 peptide sequence), Rabbit anti-MDA5 (IBL), Rabbit anti-Lamin B1 (Abcam), Mouse anti-Calnexin (Abcam) and Mouse anti-α-Tubulin (Cell signaling).

Immunofluorescence analysis: Immunofluorescence analysis was performed essentially as described (Lee et al., 2016). Briefly, cells seeded on collagen coated 24-mm coverslips were fixed with 3% paraformaldehyde and permeabilized with 0.2% Triton-X 100 in PBS. Cells were then incubated with mouse monoclonal antibody AR1 specific to IRF3 (Rustagi et al., 2013) and Rabbit anti-human NTCP (Invitrogen), followed by Alexa Flour 594-, or 488- conjugated specific secondary antibody, respectively (Invitrogen) and 4′,6-diamidino-2-phenylindole (DAPI) incubation. After immunostaining, coverslips were mounted with prolong Gold anti-fade reagent (Life Technologies) and images collected by Nikon Elipse-Ti confocal microscopy.

Cytotoxicity assays: Cytotoxicity of each treatment was measured with CellTiter-Glo Luminescent cell viability assay kit and controls (Promega) that determine the number of viable cells in culture-based quantitation of ATP present an indicator of metabolically active cells (Edwards et al., 2019). The plates were read using a luminescence plate reader (Berthold) and the relative luminescence unit (RLU) data generated from each well was calculated as percent signal compared to the untreated control. And values were expressed as CC_{50} values (50% cytotoxic concentration; the concentration of compound or poly-U/UC PAMP resulting in 50% reduction of absorbance compared to untreated cells, respectively). Tests were carried out in triplicate and each experiment was repeated three times. For the purpose of calculating selectivity index (SI), CC_{50} values greater than 40 were assigned the maximum value of 40. The selectivity index (SI) of compound was calculated as followed: $SI = CC_{50}/IC_{50}$.

HBV entry assay and cell fractionation: Cells were inoculated with HBV in presence of 4% PEG for 6 hours at 4°C. To assess HBV entry, inoculum was removed by washing with PBS that included proteinase K and cells were shifted to 37°C post-attachment. After incubation and treatment, the cells were lysed in a hypotonic buffer (100 mM HEPES, 15 mM $MgCl_2$, 100 mM KCL and Nonidet P-40), and homogenized with a dounce homogenizer. The cytoplasmic fraction was separated from nuclei pellet by centrifugation (6,000×g for 5 min at 4 °C). Nuclei pellet was resuspended in extraction buffer (20 mM HEPES, 15 mM $MgCl_2$, 420mM NaCl, 0.2 mM EDTA and 25% (v/v) Glycerol including DTT and protease inhibitor cocktail). Each cellular fraction was mixed with 1% SDS (v/v) and protein-free DNA was extracted using the Hirt extraction method.

ELISA: For ELISA, supernatant from cells were collected, centrifuged at 10,000 x g for 5 minutes, and liquid fraction recovered for analysis. HBsAg ELISA were performed on the recovered supernatant using the Hepatitis B virus s Antigen (HBsAg) Detection Kit (Cell BioLabs, INC.) following the manufacture's instructions.

cccDNA half-life analysis model: To analyze the decay of cccDNA under treatment, we employed the following mathematical model $C(t) = C(0)$ if $t \leq \tau$ otherwise $C(t) = C(0)e^{-\lambda(t-\tau)}$, where $C(t)$ is

the amount of cccDNA at time *t* post-treatment, *C(0)* is the cccDNA at the start of treatment, λ is the rate of decay of cccDNA and τ is the delay before therapy causes a decay in cccDNA. By simultaneously fitting the data from the three replicates under each of the four treatments, we estimated λ and τ using MATLAB R2017b. The half-life of cccDNA is calculated as ln (2)/ λ and reported in Figure S5. Using the function nlparci in MATLAB, which is based on the method of asymptotic normal approximation of the least squares estimator (Vandeginste, 1989), the 95% confidence interval of the parameters λ and τ were estimated and reported Figure S5.

Quantification and Statistical analysis

Statistical analyses were performed using Graphpad Prism software with multiple comparison. Continuous variable was reported as mean ± standard deviation (SD). For all tests, p values ≤ 0.05 were considered as statistically significant

Supplemental References

GUO, F., ZHAO, Q., SHERAZ, M., CHENG, J., QI, Y., SU, Q., CUCONATI, A., WEI, L., DU, Y., LI, W., CHANG, J. & GUO, J. T. 2017. HBV core protein allosteric modulators differentially alter cccDNA biosynthesis from de novo infection and intracellular amplification pathways. *PLoS Pathog,* 13**,** e1006658.

GUO, H., JIANG, D., ZHOU, T., CUCONATI, A., BLOCK, T. M. & GUO, J.-T. 2007. Characterization of the Intracellular Deproteinized Relaxed Circular DNA of Hepatitis B Virus: an Intermediate of Covalently Closed Circular DNA Formation. *Journal of Virology,* 81**,** 12472-12484.

KO, C., LEE, S., WINDISCH, M. P. & RYU, W.-S. 2014a. DDX3 DEAD-Box RNA Helicase Is a Host Factor That Restricts Hepatitis B Virus Replication at the Transcriptional Level. *Journal of Virology,* 88**,** 13689-13698.

KO, C., SHIN, Y.-C., PARK, W.-J., KIM, S., KIM, J. & RYU, W.-S. 2014b. Residues Arg703, Asp777, and Arg781 of the RNase H Domain of Hepatitis B Virus Polymerase Are Critical for Viral DNA Synthesis. *Journal of Virology,* 88**,** 154-163.

WATASHI, K., LIANG, G., IWAMOTO, M., MARUSAWA, H., UCHIDA, N., DAITO, T., KITAMURA, K., MURAMATSU, M., OHASHI, H., KIYOHARA, T., SUZUKI, R., LI, J., TONG, S., TANAKA, Y., MURATA, K., AIZAKI, H. & WAKITA, T. 2013. Interleukin-1 and tumor necrosis factor-alpha trigger restriction of hepatitis B virus infection via a cytidine deaminase activation-induced cytidine deaminase (AID). *J Biol Chem,* 288**,** 31715-27.

GRIPON, P., RUMIN, S., URBAN, S., LE SEYEC, J., GLAISE, D., CANNIE, I., GUYOMARD, C., LUCAS, J., TREPO, C. & GUGUEN-GUILLOUZO, C. 2002. Infection of a human hepatoma cell line by hepatitis B virus. *Proc Natl Acad Sci U S A,* 99**,** 15655-60.

ISHIDA, Y., YAMASAKI, C., YANAGI, A., YOSHIZANE, Y., FUJIKAWA, K., WATASHI, K., ABE, H., WAKITA, T., HAYES, C. N., CHAYAMA, K. & TATENO, C. 2015. Novel robust in vitro

hepatitis B virus infection model using fresh human hepatocytes isolated from humanized mice. *Am J Pathol,* 185**,** 1275-85.

ESSER-NOBIS, K., AARREBERG, L. D., ROBY, J. A., FAIRGRIEVE, M. R., GREEN, R. & GALE, M., JR. 2019. Comparative Analysis of African and Asian Lineage-Derived Zika Virus Strains Reveals Differences in Activation of and Sensitivity to Antiviral Innate Immunity. *J Virol,* 93.

NI, Y., LEMPP, F. A., MEHRLE, S., NKONGOLO, S., KAUFMAN, C., FALTH, M., STINDT, J., KONIGER, C., NASSAL, M., KUBITZ, R., SULTMANN, H. & URBAN, S. 2014. Hepatitis B and D viruses exploit sodium taurocholate co-transporting polypeptide for species-specific entry into hepatocytes. *Gastroenterology,* 146**,** 1070-83.

PROBST, P., GRIGG, J. B., WANG, M., MUNOZ, E., LOO, Y. M., IRETON, R. C., GALE, M., JR., IADONATO, S. P. & BEDARD, K. M. 2017. A small-molecule IRF3 agonist functions as an influenza vaccine adjuvant by modulating the antiviral immune response. *Vaccine,* 35**,** 1964-1971.

IADONATO, S. P., KAISER, S., BEDARD, K. M., FOWLER, K. W. & MADU, I. 2018. *Anti-viral compounds, pharmaceutical compositions, and methods of use thereof*. US patent application.

LOO, Y. M., FORNEK, J., CROCHET, N., BAJWA, G., PERWITASARI, O., MARTINEZ-SOBRIDO, L., AKIRA, S., GILL, M. A., GARCIA-SASTRE, A., KATZE, M. G. & GALE, M., JR. 2008. Distinct RIG-I and MDA5 signaling by RNA viruses in innate immunity. *J Virol,* 82**,** 335-45.

SAITO, T., OWEN, D. M., JIANG, F., MARCOTRIGIANO, J. & GALE, M., JR. 2008. Innate immunity induced by composition-dependent RIG-I recognition of hepatitis C virus RNA. *Nature,* 454**,** 523-7.

KELL, A., STODDARD, M., LI, H., MARCOTRIGIANO, J., SHAW, G. M. & GALE, M., JR. 2015. Pathogen-Associated Molecular Pattern Recognition of Hepatitis C Virus Transmitted/Founder Variants by RIG-I Is Dependent on U-Core Length. *J Virol,* 89**,** 11056-68.

CAI, D., NIE, H., YAN, R., GUO, J. T., BLOCK, T. M. & GUO, H. 2013. A southern blot assay for detection of hepatitis B virus covalently closed circular DNA from cell cultures. *Methods Mol Biol,* 1030**,** 151-61.

LEE, S., KIM, W., KO, C. & RYU, W. S. 2016. Hepatitis B virus X protein enhances Myc stability by inhibiting SCF(Skp2) ubiquitin E3 ligase-mediated Myc ubiquitination and contributes to oncogenesis. *Oncogene,* 35**,** 1857-67.

RUSTAGI, A., DOEHLE, B. P., MCELRATH, M. J. & GALE, M., JR. 2013. Two new monoclonal antibodies for biochemical and flow cytometric analyses of human interferon regulatory factor-3 activation, turnover, and depletion. *Methods,* 59**,** 225-32.

EDWARDS, T. C., MANI, N., DORSEY, B., KAKARLA, R., RIJNBRAND, R., SOFIA, M. J. & TAVIS, J. E. 2019. Inhibition of HBV replication by N-hydroxyisoquinolinedione and N-hydroxypyridinedione ribonuclease H inhibitors. *Antiviral Res,* 164**,** 70-80.

VANDEGINSTE, B. 1989. Nonlinear regression analysis: Its applications, D. M. Bates and D. G. Watts, Wiley, New York, 1988. ISBN 0471-816434. Price: £34.50. *Journal of Chemometrics,* 3**,** 544-545.